

Hierarchically structured composites and porous materials from soft templates: fabrication and applications

Benjamin R. Thompson,^a Tommy S. Horozov,^a Simeon. D. Stoyanov,^{b,c,d} and Vesselin N. Paunov^{*a}

Received 00th January 20xx,
Accepted 00th January 20xx

DOI: 10.1039/x0xx00000x

rsc.li/materials-a

Recent experimental methods for fabrication of hierarchically porous and structured composites are reviewed. The main focus is on recent examples of how different soft templating materials, like emulsions, surfactant phases, breath figures, biological templates, liquid marbles and hydrogel bead slurries can be used to fabricate hierarchically porous materials with tuneable porosity, pore sizes and ratio of different sized pores. Approaches for tuning the physical properties (mechanical, thermal, acoustical) of these innovative materials as well as controlling the porosity, pore size and microstructure are discussed. We also show a variety of applications of hierarchically structured composites in catalysis, energy storage, usage and conversion, removal of pollutions, sensors, biomaterials, smart soaps, and structuring of consumer products.

Introduction

Hierarchically structured porous composites have been subject to increased interest due to their unique properties and various applications.^{1–4} A range of methods for preparation of these materials have already been proposed recently and reviewed in the literature.^{2–12} Porous materials are classified as micro-, meso- or macroporous if their pore diameter is below 2 nm, 2–50 nm or larger than 50 nm, respectively.¹³

In general, hierarchically structured/porous materials are broadly defined as those containing organised structural elements/ pores on multiple length scales.^{148–152} This could be a combination of micro-mesopores, micro-macropores, meso-macropores or two different length scale of the same type pores (for example macro-macro with 100 nm and 100 μm pore diameters). Furthermore, tri-modal pore size distributions (micro-meso-macro) have also been demonstrated.¹⁴

In the recent literature related mainly to open pore systems (such as zeolites, membranes, etc.) in which the flow and transport through the material are of paramount importance, a narrower definition of hierarchy has been adopted, that in the ‘narrow’ sense, one has to consider the existence of an interplay between the different pore levels before one can name the overall pore system ‘hierarchical’.¹⁵³ The interconnectivity pattern between systems of differently sized pore levels, allows the hierarchically porous materials to be put in two sub-categories: Hierarchy-type I: in which each level subdivides into

several species of a next level, and Hierarchy-type II, of interconnected pore systems where small pores branch off from a continuous large pore.¹⁵³

Another type of hierarchical porosity is where the porosity is graded i.e. a continuous increase or decrease in pore dimensions along one direction. Such materials have been exploited for their enhanced sound absorbing properties when the pore size decreases along the direction of sound wave propagation. These types of porous structures have a steady increase in resistance to airflow due to decreasing pore size.¹⁵ There are many different types of pores, of which the most well-known are open and closed pores. IUPAC have classified pores according to their availability to an external fluid. In Figure 1, (a) shows a closed pore i.e. a pore that is isolated from neighbouring pores. The pores shown in Figure 1 (b)–(f) are open pores as they are open to the surface of the material. These can be classified as through pores (e) or dead-end pores (b) and (f). Further classification can be done from the pore shape; they can be cylindrical (through open (e) or dead-end open (f)). They can also be ink-bottle shaped (b) or funnel shaped (d). Finally, (g) shows the roughness of the surface of the material. This can be classed as a type of pore if the depth is greater than the width. A significant amount of research is being performed on materials with structural hierarchy because of their immense potential in a large number of applications. The combination of a large surface area due to micropores and easier mass transport due to the presence of meso- or macropores can lead to materials with superior properties to those with a single pore size distribution.¹⁶

Biological materials (i.e. wood, bone or grass) produced through long-term evolution to be optimal for their purpose are often found to be hierarchically structured.¹⁷ Many of these materials have an astounding efficiency, which is believed to be due to a functional adaptation of all levels of the hierarchical structure.¹⁸

^a Department of Chemistry and Biochemistry, University of Hull, Hull, United Kingdom; Correspondence: V.N.Paunov@hull.ac.uk; tel: +44 1482 465660.

^b Unilever R&D Vlaardingen, Olivier van Noortlaan 120, 3133 AT Vlaardingen, the Netherlands.

^c Laboratory of Physical Chemistry and Soft Matter, Wageningen University, 6703 HB Wageningen, The Netherlands.

^d Department of Mechanical Engineering, University College London, Torrington Place, London WC1E 7JE, UK.



Benjamin R. Thompson

consumer products.

Dr Benjamin Thompson received his PhD degree in Physical Chemistry from the University of Hull in 2017. Currently, he is a Post-doctoral fellow at the Department of Chemical and Biomolecular Engineering at the University of Maryland. His research interests include colloids, hydrogels, templating methods, porous materials for sound and heat insulation, structuring of food and



Tommy S. Horozov

Professor at the Department of Materials Chemistry, University of Vienna, Austria. His research interests include anisotropic particles, metamaterials, particles at interfaces, Pickering emulsions and foams, surfactants, colloids, porous polymers and composite materials.

Dr Tommy Horozov holds a PhD degree in Physical Chemistry from the University of Sofia, Bulgaria. He joined the University of Hull, UK as a Post-doctoral research fellow in 2000 and received the EPSRC Advanced Research Fellowship award (2006-2011). Currently, he is a Senior Lecturer at the University of Hull and a Visiting



Simeon D. Stoyanov

Interfaces at Unilever R & D in Vlaardingen and a Visiting Professor in University of Wageningen, The Netherlands and University College London, UK. His research interests cover various topics of soft-condensed matter, materials science, self-assembly, surface science of liquid–liquid interfaces, foams and emulsions, physical-chemistry of digestion and encapsulation.

Professor Simeon D. Stoyanov received his PhD from Essen University, Germany. He has worked in the Laboratory of Chemical Physics and Engineering in University of Sofia, Bulgaria, as a visiting scientist at the École Normale Supérieure, Paris, France, University of Erlangen and Henkel R & D in Dusseldorf, Germany. Currently he is a Senior Scientist in Colloids and



Vesselin N. Paunov

In 2000 he took an academic post at the University of Hull, UK where he is currently a Professor of Physical Chemistry and Advanced Materials at the School of Mathematics and Physical Sciences (Chemistry). His present research interests include formulation science, microencapsulation, triggered release of actives, antimicrobial nanoparticles, colloid antibodies for cell shape recognition, selective targeting of cells, whole cell bioimprinting techniques and bioimprint-cell interactions.

Professor Vesselin N. Paunov received his PhD in Physical Chemistry in 1997 from the University of Sofia, Bulgaria. He worked as a visiting researcher at the Universities of Patras, Greece, and Erlangen, Germany and as a postdoctoral researcher at the University of Delaware.

Hierarchical structuring of porous materials can mimic natural materials in an attempt to obtain optimal structures and can lead to novel materials with the possibility of the functionalisation of each level of porosity.

In the present review, we consider recent advances in the methods for preparation of composite materials with hierarchical structure and porosity and put the focus on novel practical applications. Our main focus is on the methods using soft templates (e.g. hydrogels) due to their advantages over hard solid templates such as colloid crystals or polymers which are also briefly considered for comparison.

Methods of production of materials with hierarchical structure and porosity

Whilst there are many techniques to produce hierarchically porous materials, it is difficult to classify them into separate sections as they are commonly a combination of multiple techniques. However, the next part of this review will aim to cover some of the widely used templating methods for synthesising materials with multimodal porosity (see Figure 2). A thorough review on other preparation methods can be found elsewhere.^{10,153}

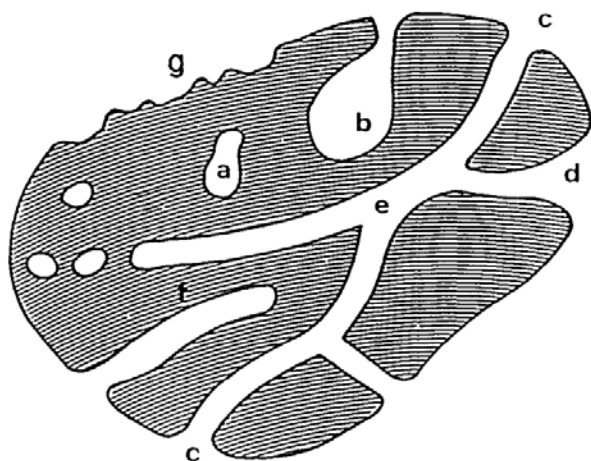


Figure 1. Schematic cross section of a porous material showing (a) - a closed pore, (b) - an open ink-bottle shaped open pore, (c) - a through open pore, (d) - a funnel shaped open pore, (e) - an open pore, (f) - a dead-end open pore and (g) - the surface roughness which can be classed as a pore if it is deeper than wide. Reproduced with permission from Ref. 13. Copyright 1994, IUPAC.

Surfactant templating

Some of the early techniques to produce materials with hierarchically porous structures involved the use of surfactant templates. Through careful control of the phase separation of two surfactants dissolved in an aqueous medium, it is possible to use these surfactant assemblies for fabricating a hierarchically structured material. The choice of surfactants is of utmost importance as their interaction determines whether they can be used to introduce hierarchical porosity. Sel and Smarsly discussed the possible outcomes of porous materials fabrication by mixing two different surfactants in solution.²⁰ The self-assembly of the surfactants into micellar structures will occur at concentrations above the critical micelle concentration. This takes place to lower the free energy of the system by reducing the contact between the hydrophobic hydrocarbon regions and the surrounding water.²¹ Whilst this method seems simple, mixing of micelles is the issue holding it back, with no current examples of using a three surfactant system as a template to produce a material with a trimodal mesoporous structure. This approach is limited by the availability of data for phase diagrams of mixed surfactant systems. If trimodal porosity is required, a combination of surfactant templating and another technique to introduce porosity on a different length scale would be needed. One group utilised a block copolymer surfactant, an ionic liquid surfactant and polystyrene (PS) microspheres as templates to produce a material with hierarchical porosity with pores on three different length scales.²²

Breath figures templating

The fog that forms when water vapour condenses upon contact with a cold surface is known as a breath figure (BF). An everyday example that led to its name is breath on a window. These were first utilised for the preparation of structured films in 1994.²³

The general procedure is encouraged by evaporation of the solvent of a polymer solution. The process of evaporative cooling causes water droplets to condense on the surface into a well ordered hexagonal array which is stabilised by the polymer in solution. If the solvent has a higher density than water, the droplets will only structure the surface. Conversely, if the solvent is less dense than water, the droplets will propagate through the polymer solution and introduce porosity upon drying.¹⁰ This method is attractive due to using water as the template and because of the possibility of tuning the pore size by controlling the preparation conditions. Whilst the preparation methods of materials structured by BFs are fairly simple, the theory behind them is not, due to complex mass and heat transfer mechanisms. A thorough review on BFs can be found elsewhere.²⁴ BFs have been used to prepare hierarchically structured films. One method involved addition of trioctylphosphine oxide (TOPO) ligand stabilised CdSe nanoparticles to a PS solution in chloroform. It was evaporated at room temperature and 80% humidity. The drying of the water droplets produced pores that were decorated with CdSe nanoparticles trapped at the polymer-air interface, resulting in a hierarchically structured PS film.²⁵

Freeze drying

Freeze drying is the process of freezing a solution, usually in liquid nitrogen, then removing the frozen solvent by sublimation at a pressure and temperature below its triple point.²⁷ This process has been exploited for the preparation of porous and hierarchically porous materials and is known as ice-templating.¹⁰ The porous structure can be varied by controlling the freezing rate, initial freezing temperature, solution concentration and direction of freezing.^{27,28}

A binary colloid system has been ice templated to obtain a hierarchically structured material. It involved the dispersion of submicron size silica (SiO₂) particles into a SiO₂ sol. After subsequent gelation and freeze-drying, a hierarchically structured material was obtained.²⁹ This technique has many advantages, the first being the use of environmentally friendly water ice as the pore inducing template. It can also be applied to many types of materials and can be used for biological applications. Thorough reviews on ice templating, also known as freeze-casting, can be found elsewhere.^{27,30}

Colloidal crystal templating

A colloidal crystal contains a large number of monodisperse colloidal particles arranged in a three-dimensional uniform array.³¹ The most common colloidal crystal structure is the face centred cubic (FCC), however there are reports of other lattice geometries.^{32,33} These colloidal crystals can be used as sacrificial hard templates to introduce well-ordered and monodisperse pores into materials (Figure 3). A general technique, described in 1997, was the preparation of a PS latex solution and then allowing it to form a crystal structure on a membrane due to sedimentation. It was subsequently soaked with hexadecyltrimethylammonium bromide (HTAB) solution to hydrophobise the latex particles which would induce polymerisation of a SiO₂ sol.

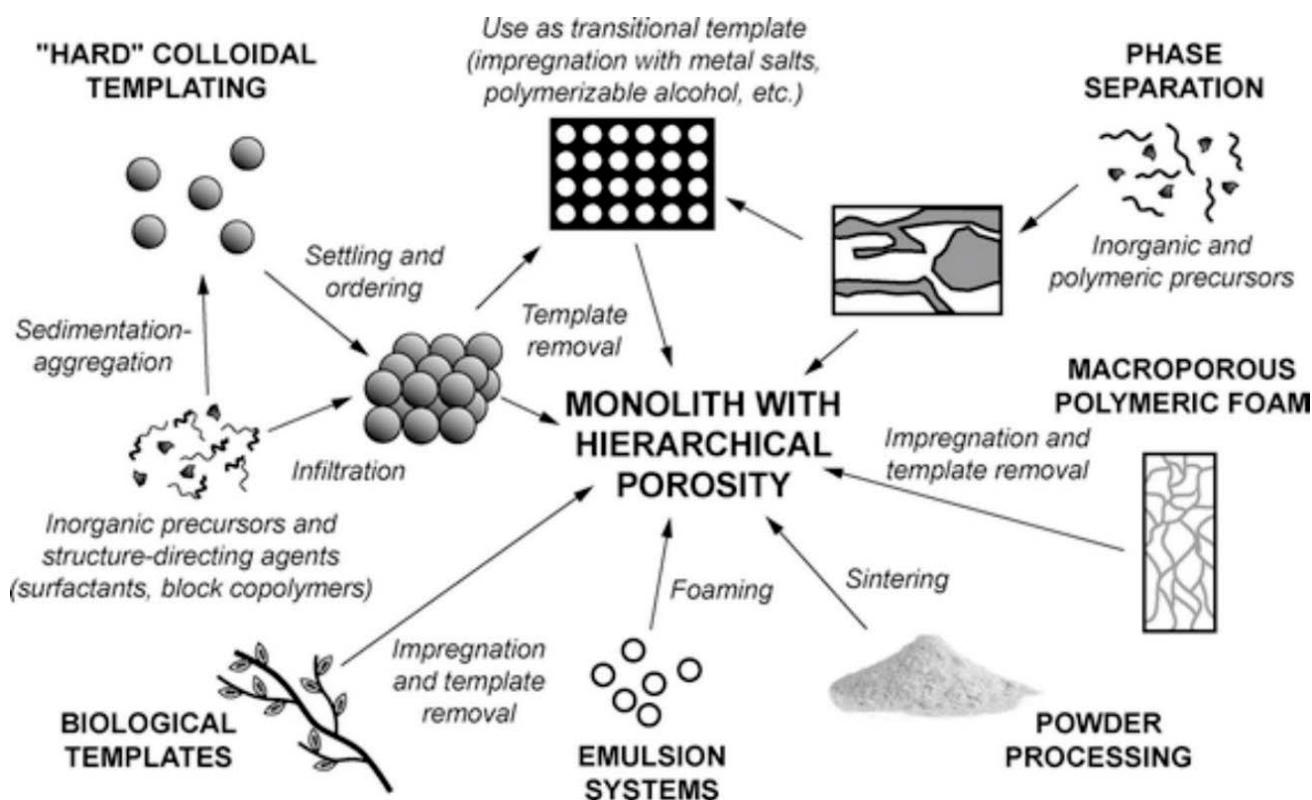


Figure 2. Schematic overview of some of the current methods for production of hierarchically porous materials.¹⁹ Reproduced with permission from Ref. 19. Copyright 2010, Springer.

The excess HTAB was removed by washing with water which was followed by infiltration of the colloidal crystal with a SiO_2 sol. This was left to gel, dried under vacuum and finally the latex particles were removed by heating to $450\text{ }^\circ\text{C}$ for four hours to obtain a porous SiO_2 monolith.³⁴ This method can be further developed by using two different sized latex particles,³⁵ or combined with other methods to introduce porosity such as surfactant templating or zeolites to prepare hierarchically porous materials.^{36,37} Velev *et al.* have utilised this method to obtain hierarchically porous gold by preparing a solution of PS latex particles and gold nanoparticles.

They were allowed to sediment on a membrane where the PS formed a colloidal crystal structure and the gold nanoparticles were within the interstitial holes. PS was removed by heating, thus yielding macroporous gold. However, if acid or trichloromethane was used to remove the PS, hierarchically meso-macroporous gold was obtained.³⁸ This approach allows for a great control over the size and monodispersity of the pores but its disadvantage is that the template particles have to be destroyed in the final stages of material preparation.

Biological templating

Another templating technique involves the use of natural plants as templates. This is a clever approach as hierarchically porous structures in nature have pores that are well ordered and have a small pore size distribution. For example, a SiO_2 sol was

prepared and mixed with various parts of plant structure which had various types of porosities. Pith was used that had pores that decreased in size from edge to centre, while xylem has hierarchical porosity and epidermis had a single level of porosity. Upon drying and calcination of the sol, the SiO_2 monolith had a porous structure that represented the template used.³⁹

Emulsion templating methods

Emulsion templating is an effective and widely used technique for preparing porous materials with tuneable porosity, pore sizes and connectivity. For example, high porosity polymeric materials can be easily produced from water-in-oil high internal phase emulsion (HIPE) templates^{40,143,144} (i.e. emulsions with a volume fraction of the dispersed phase greater than 0.74) stabilised by surfactants,^{40, 143} solid particles alone⁴¹ or mixtures of both.⁴² The polymerisation of the continuous oil phase and subsequent evaporation of the dispersed water droplets produce macroporous polymers typically with polydisperse pore sizes in the micrometre range.

HIPEs have also been employed as templates for preparation of hierarchically porous materials. Through control of the preparation conditions, it is possible to obtain bimodal droplet sizes which leads to a hierarchical pore size distribution. A study has shown that low surfactant concentrations and short homogenisation times leads to polydisperse water droplets.⁴³

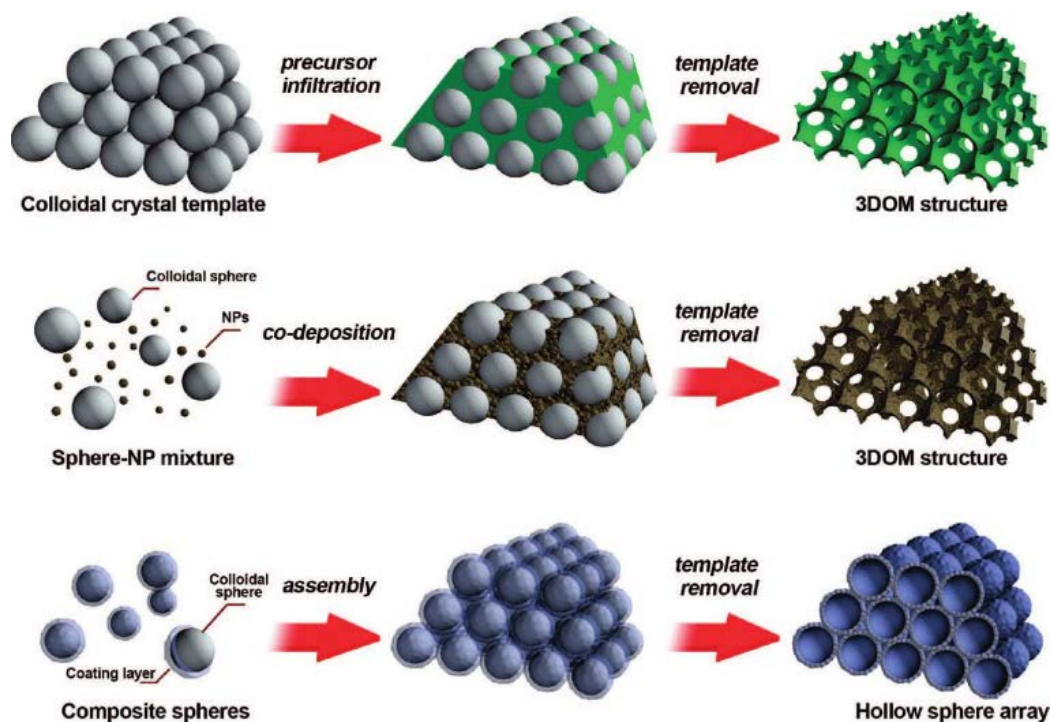


Figure 3. Three different schematics showing examples of colloidal crystal templating. Reprinted with permission from Ref. 32. Copyright 2008 American Chemical Society.

They prepared a HIPE of aqueous CaCl_2 solution dispersed in a continuous phase consisting of styrene, divinylbenzene (DVB), Hypermer 2296 surfactant and azobisisobutyronitrile (AIBN, a free radical initiator). After preparation, it was immediately polymerised by heating to 70 °C for 24 hours. Finally, it was dried in a vacuum oven to obtain a hierarchically porous polymerised HIPE (polyHIPE).⁴³ There are many other examples of the use of polyHIPEs to obtain hierarchically porous materials.^{44,45}

Polymer templating methods

Hierarchically structured polymers can be employed as sacrificial templates for the production of porous materials. The mixing of such structures with a scaffold material, followed by the subsequent removal of the template can yield materials with a hierarchical structure that reflects the initial microstructure of the templates. Monodisperse PS latex particles can be prepared with a variety of sizes and surface functionalities. Figure 4 shows how combining two different size PS particles to prepare hierarchically structured PS templates could be utilised to prepare a porous material with two different monodisperse pore sizes.⁴⁶ They functionalised the surface of small PS particles (80 nm diameter) with NH_2 groups and large PS particles (1.5 μm diameter) with COOH groups. The small PS particles assembled around the surface of the large PS particles when they were mixed together (small in excess) due to electrostatic interactions. A coupling reaction was used to fix them in place. They were then mixed with a SiO_2 sol, followed by drying and then removal of the templates by heating to 540 °C for three hours. This produced a hierarchically

porous material with a raspberry-like internal structure imparted by the template.⁴⁶ Another way polymer templating can be used to produce hierarchically porous materials is through the infiltration of a polymer gel network by nanoparticles. It has been demonstrated by Fe_3O_4 nanoparticles infiltrating into poly(acrylic acid).

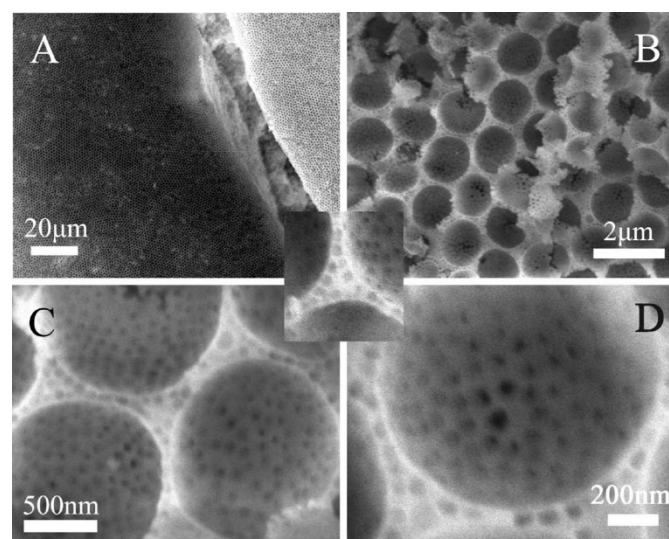


Figure 4. Hierarchically porous SiO_2 produced using raspberry-like PS particles. Reprinted with permission from Ref. 46. Copyright 2010 American Chemical Society.

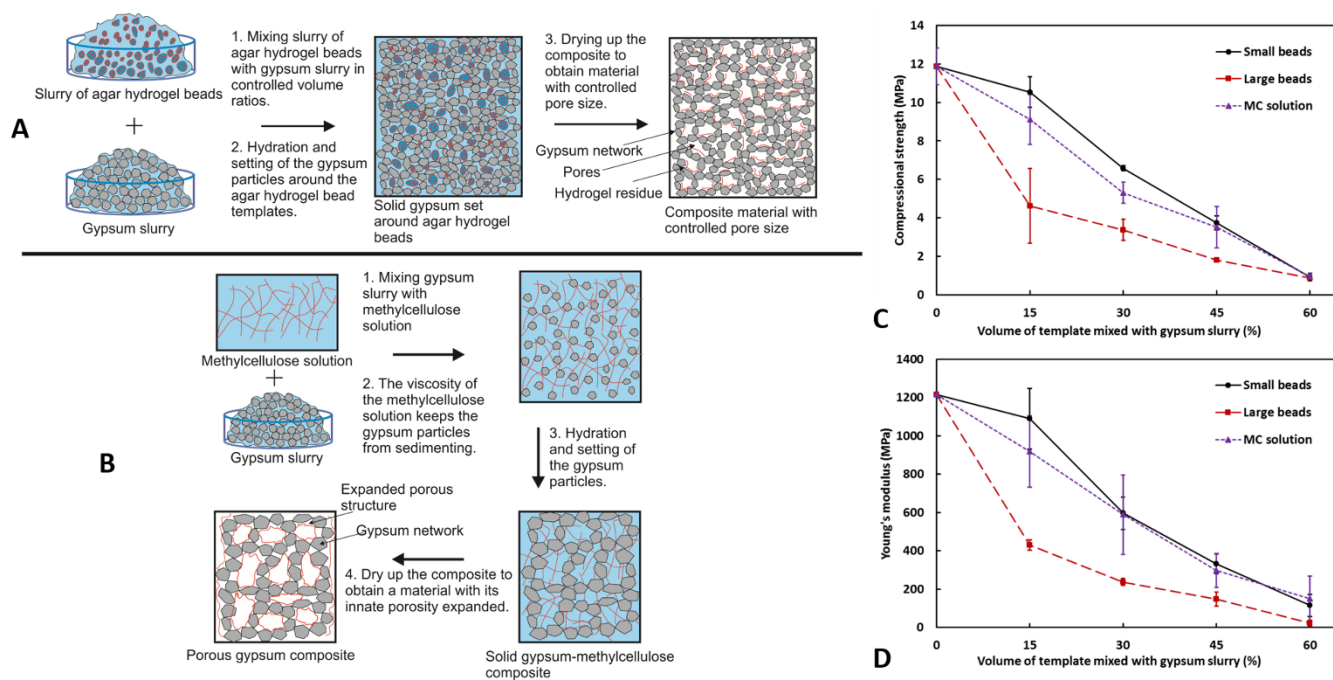


Figure 5. Schematics of (A) the hydrogel beads templating technique^{123,125, 126} and (B) the viscous trapping method^{126,127} for production of hierarchically porous composites from gypsum or cement. The viscous trapping utilises methyl cellulose (MC) solution to control the porosity and pore size of gypsum composites. Gypsum (or cement) slurry is mixed with either small hydrogel beads, large hydrogel beads or MC solution in controlled volume ratios. Subsequent setting of the gypsum (or cement) slurry and then drying of the composite produces materials with controlled porosity and tuneable microstructures. The pore size distribution reflects the size distribution of the hydrogel slurry used for the templating process. Mixing slurries of small and large hydrogel bead and gypsum slurries allows fabrication of hierarchically porous composites with unique properties. (C) Compressional strength and (D) Young modulus of the porous gypsum composites obtained with these methods versus of percentage of the hydrogel templating phase (hydrogel slurry or MC solution). The compressional strength and the Young modulus depend strongly on the hydrogel beads size with the once of smaller size being stronger. Reproduced with permission from Ref. 126. Copyright 2018, Elsevier.

Upon removal of the polymer by heating in air, the nanoparticle structure was left intact and formed a hierarchically porous material.⁴⁷ Similar to the colloid crystal templating, the need for removal (dissolution) of the solid polymer template is amongst the disadvantages of this method.

Hydrogel templating methods

Recently, a cheap, easy and environmentally friendly method using hydrogel bead templates for introducing porosity into a material was proposed by Rutkevicius *et al.*^{123, 124} The method also gives a large amount of control over both the porosity and pore size. A hydrogel bead templating technique that involved the use of gellan or polyacrylamide hydrogel beads as templates to introduce porosity into a variety of materials has been reported.^{123, 125} By combining slurries of the matrix material and hydrogel beads in controlled volume ratios, followed by subsequent curing and then drying, porous materials were obtained with a porosity controlled by the volume of hydrogel beads used. Furthermore, the average pore size of the composite was set by the size of the hydrogel beads used. This method was extended further to make hierarchically porous gypsum composites by using agar hydrogel beads of different sizes as the templates. The use of agar hydrogel instead of gellan or polyacrylamide gels is due to the gelling properties of agar, agarose, being a non-ionic polymer that does not interact with the calcium ions from the gypsum slurry, which allows for a better control during the formulation of these composites.¹²⁵

Thompson *et al.*¹²⁶ extended further this approach by developing two different methods to formulate hierarchically porous gypsum composites, both of which are, inexpensive, work at room temperature and give a large amount of control over the composite microstructure (Figure 5).

Figures 5A and 5B show schematically the process of hydrogel beads templating for fabrication of porous gypsum composites. The hydrogel bead templating method involved introducing a slurry of hydrogel beads as templates into a gypsum slurry that, upon drying, left pores reproducing their size (Figure 5A). The overall porosity reflected the volume percentage of hydrogel bead slurry used. Using mixtures of large and small hydrogel beads in controlled volume ratios as templates, they produced hierarchically porous gypsum composites that had tailorable microstructures at the same overall porosity. The viscous trapping method involved an aqueous solution of a thickening agent, methylcellulose, during the setting process of an aqueous gypsum slurry (Figure 5B). The methylcellulose solution traps the hydrated gypsum particles in solution and stops their sedimentation as the continuous gypsum network forms; allowing for the formation of an expanded microstructure. This method allows a high degree of control over porosity by the volume percentage of methylcellulose solution used. The mechanical strength of the porous composites showed a decrease as the porosity increased (Figure 5C and 5D).

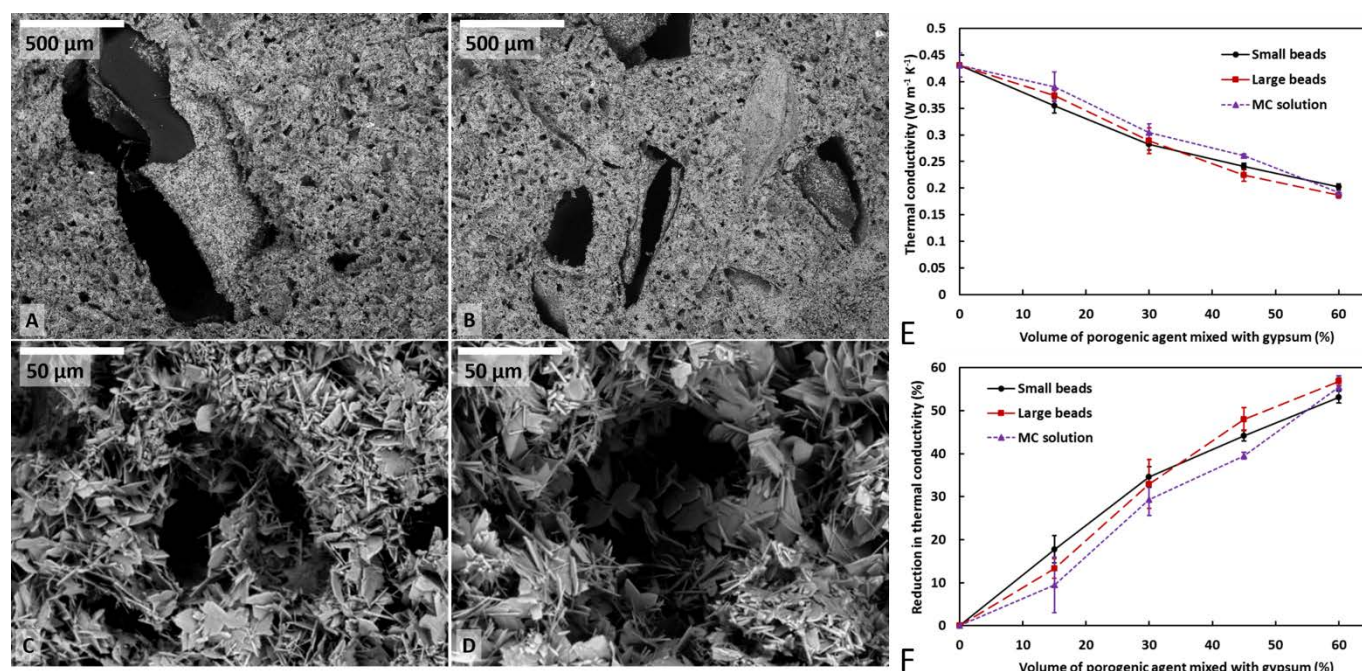


Figure 6. SEM images of hierarchically porous gypsum composites produced using a dual size hydrogel bead templating process (A) and (B) or a combination of small hydrogel beads and MC solution (C) and (D).¹²⁶ (A) has a porosity of 50% that was induced by 30% large beads and 20% small beads whereas (B) has the same porosity but it was induced by 20% large beads and 30% small beads. The sample seen in (C) has a porosity of 50% from 10% MC solution and 40% small beads and (D) shows a sample produced with 10% small beads and 40% MC solution. (E)-(F) The thermal conductivity of such porous gypsum composites seems to be weakly dependent on the size of the hydrogel beads but strongly depends on the overall porosity. Reproduced with permission from Ref. 126. Copyright 2018, Elsevier.

The composites with smaller pores had increased compressional strength and Young's modulus compared to the ones with large pores, at constant porosity. The hierarchically porous gypsum composites showed an intermediate Young's modulus and an increased compressional strength. Both the hydrogel slurry templating and the viscous trapping methods (Figure 5) can also be used to introduce hierarchical porosity in cement, ceramics, food, home and personal care products and other composite materials of similar setting process.

Thompson *et al.*¹²⁶ studied how the thermal conductivity and mechanical properties of the porous gypsum composites vary with porosity and pore size. They reported that the thermal insulation properties of porous composites prepared by templating with hydrogel slurries did not depend on the size of the hydrogel beads used but on the overall porosity. The thermal conductivity of the hierarchically porous gypsum composites produced by both the hydrogel templating and the viscous trapping methods decreased with the increase of the overall porosity. However the thermal conductivity was not dependent on the composition of the pores with small and large pores giving very similar results at the same porosity (Figure 6).

Liquid marbles templating

Rutkevicius *et al.*¹³¹ designed a new method for preparation of salt-hydrogel marbles from salt microcrystals and aqueous solution of gelling agents (Figure 7). Their method is based on

gelling droplets of hot aerosolised solution of a gelling agent in a cold air column and the deposition of the obtained hydrogel microbeads over a bed of microcrystalline salt powder which forms a particle layer around them. The produced salt-hydrogel marbles were separated from the excess of salt microcrystals by sieving and upon drying of the hydrogel cores yielded hollow-shell salt microcapsules in which big pores (cavities) were surrounded by microporous salt shells. This method allows fabrication of marbles from aqueous solutions and hydrophilic particles which is a challenge for the other methods for preparation of liquid marbles, where hydrophobic particles are used as stabilisers. These authors show that when hydrogel microbeads are used instead of liquid drops, hollow-shell salt microcapsules can be produced upon drying of the salt marbles. In contrast, liquid drops of gelling agent yield porous salt granules without apparent cavity due to the complete capillary penetration of the liquid within the bed of hydrophilic salt microcrystals (Figure 7a and 7b). The application of this method was demonstrated for the fabrication of salt-hydrogel marbles by producing edible hollow-shell salt microcapsules which could be used in the food industry for the development of salt-based seasonings of reduced salt content.¹³¹ The presence of hollow-shell coated with salt microcrystals provides a potential advantage of such microcapsules compared to the use of table salt.

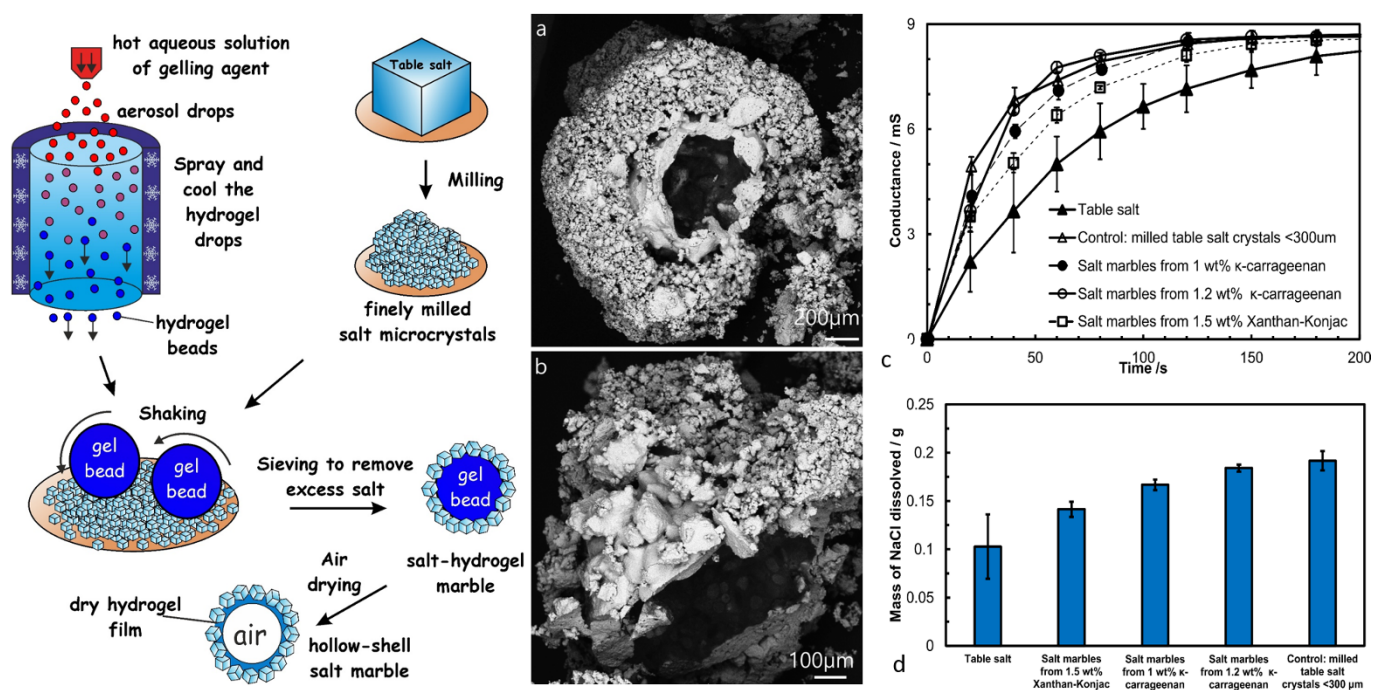


Figure 7. LHS: Schematic representation of the method used to produce salt-hydrogel marbles and hollow-shell particles. A hot hydrogel solution is atomized, producing aerosol droplets, which are flash-gelled by passing through cold air column. The formed aerosol hydrogel beads are collected over a bed of finely milled salt microcrystals. As the salt bed is vibrated, a layer of salt crystals is deposited on the rolling hydrogel beads which forms hydrogel-salt marbles. These are then removed from the excess salt by sieving, and further dried to produce hollow-shell salt marbles. (a)-(b) SEM images of dried salt marbles (crack open) produced with 1.0 wt% Xanthan-Konjac 2:1 hydrogel beads. (a-b) column inner surface temperature $\sim 6^\circ\text{C}$. (c) Conductance of the aqueous medium vs. time after the addition of a fixed amount (0.2500 g) of table salt or hollow-shell salt marbles. The table salt particles had an average mean particle diameter of $280 \pm 100 \mu\text{m}$ and the milled salt crystals were $30 \pm 20 \mu\text{m}$. (d) The mass of NaCl dissolved upon dissolution of different samples of salt or salt marbles after the addition of the sample into a fixed amount of water derived from results in (c). The higher the mass of the dissolved salt the higher is the perception of saltiness. The graph shows that compared with the ordinary non-milled table salt, higher mass and possibly saltiness feel could be delivered using salt marbles produced by hydrogel bead templating instead of the equivalent amount of table salt. Reprinted with permission from Ref 131. Copyright 2015, The Royal Society of Chemistry.

The methodology of hollow-core marbles production does not seem to be limited to hydrophilic particles for the shell structures, like the sodium chloride microcrystals, but could also be potentially applied to many other organic and inorganic particles, both hydrophilic and hydrophobic. The authors envisage that the preparation of salt marbles could be further improved by using powerful atomizers for aerosol generation from aqueous solution of higher viscosity and higher concentration of gelling agent, which would further reduce the size of the hydrogel beads. These authors demonstrate that dried salt marbles, due to their dual porosity, have superior rate of salt release compared to ordinary table salt upon dissolution in water. Hence salt marbles hold promise for possible replacement of the conventional table salt (Figure 7c and 7d). Despite the reduced salt content, salt marbles gave the same or higher rate of salt release upon dissolution which would create the same perception for “saltiness”. Hence such salt marbles could be used as a healthier alternative for reducing salt intake by consumers, through reduced amount of salt used in salt seasonings and development of healthier snack products.

Modelling of hierarchically porous composites

With the recent significant advances being made in the synthesis of hierarchically porous materials with well-defined, tuneable architectures, efforts can now be aimed towards optimisation of hierarchical structures for their role. Strategies towards the design and implementation of state-of-the-art materials should involve taking insights from theoretical and computational studies. These such studies allow for a deeper understanding of what is occurring within nano- and microstructured materials, which can be used for the rational design of a hierarchically porous material for a specific purpose. Vargas *et al.* performed molecular dynamics simulations on the transport of n-alkanes in the hierarchically porous metal-organic framework (MOF) NU-1000, which is a microporous material with mesoporous channels.¹⁴⁵ Their first finding was that the micropores were preferentially filled as they were housing more than 65% of the adsorbed molecules even though they account for less than one quarter of the volume of a unit cell. Only once the micropores were full did the distribution of molecules shift towards the mesoporous channels. It was found that this continued until the occupancy of the micro and mesochannels was proportional to their respective volumes and there was even coverage throughout the unit cell.

From comparison of density plots at different temperatures, they confirmed this was dependent on loading, not fugacity. They investigated self-diffusion of molecules within the hierarchically porous MOF and their findings revealed that maximum molecule mobility was seen at intermediate loading, which they explained by active sites hindering transport at low concentrations, and a reduction in available volume hindering transport at high concentrations. Using a finite sub-volumes approach, they applied different diffusion coefficients to the different regions of the unit cell in order to probe the dynamics of transport of small molecules through this heterogeneous framework and it was seen that the mesoporous channels provided regions of enhanced diffusion. Another group have utilized a modified lattice Boltzmann scheme for fluid transport in nanoporous materials which takes the adsorption of solutes on the solid-liquid interface into account.¹⁴⁶ After validating their model on simple hierarchical structures with known analytical solutions, they then used it to study the kinetics of adsorption and the accessibility of active sites in materials with more complex architectures. Slit pore geometries that had walls of regular grooves or disordered roughness were investigated. They demonstrated the importance of active site accessibility, which depends on the shape and connectivity of the pores as well as the fluid flow profile and velocity. Structure-property relations are of significant importance as it allows for the fine-tuning of materials with desired characteristics. One group have used a finite volume method and proposed an analytical-numerical model to predict the stiffness and strength of hollow-structured metal foams with structural hierarchy.¹⁴⁷ They investigated two structures: FCC and HCP lattices of hollow gold particles and determined that FCC foams are stiffer than HCP foams when the thickness of the hollow gold particles was low, but at higher thickness (>0.7 μm) HCP foams had a higher Young's modulus. They also showed that the relative density of the shell had a greater impact on the mechanical properties than the shell thickness. The authors envisage that while their model can predict the mechanical properties of hierarchically porous metal foams, it can also be used in further analytical-numerical studies to reveal other interesting properties.

Applications of hierarchically porous materials and hierarchically structured composites

Hierarchically structured materials have been utilised for specific applications in recent years. We outline some recent advances in these areas based on different categories of porous and composite materials.

Catalysis

A large proportion of research into materials with hierarchical porosity goes into their applications in catalysis. With catalytic processes being involved in more than 20% of all industrial processes, it is highly worthwhile to develop more efficient catalysts.¹¹ Hierarchically porous materials are well suited for this role due to their high surface area due to the presence of micropores, leading to an abundance of active sites.

Furthermore, macropores provide easier mass transport through the material due to lower pressure drops i.e. a reduction in frictional forces compared to meso- or micropores.⁴⁸ Through careful design of hierarchically structured materials, it is possible to prepare catalysts for oxygen reduction reactions (ORRs) that do not contain precious metals, yet have a comparable or superior activity to them. ORRs are very important reactions that occur at a cathode and determine the performance of fuel cells and metal-air batteries.⁴⁹ Metal organic frameworks (MOFs) have been investigated as precursors to produce porous carbon-based catalysts for ORRs. This technique allows for controllable porous structural characteristics by changing one or both of the central metal ion and the bridging electron donating molecules. Furthermore, it allows for doping of the final product by the inclusion of heteroatoms within the organic linkers. MOFs have been used to produce porous carbon-based materials previously, however their ORR activity was lower than current commercial catalysts. This is assumed to be due to low specific surface area, a microporous structure or poor electrical conductivity, or a combination of these.⁵⁰

Zeolitic imidazolate frameworks (ZIFs) are a subclass of MOF and a combination of two ZIFs have been used to produce a hierarchically porous cobalt and nitrogen co-doped carbon-based electrocatalyst. Core-shell materials with a ZIF-8 (zinc-based) core and a ZIF-67 (cobalt-based) shell were produced using a ZIF-8 seed mediated growth of ZIF-67 crystals.⁵¹ Briefly, ZIF-67 crystals were grown on ZIF-8 seeds and then they were heated at 950 °C for two hours in an argon atmosphere to produce cobalt and nitrogen co-doped hierarchically porous carbon nanopolyhedra. This was then investigated for its ORR activity and was found to be superior to a commercial platinum-based catalyst. Furthermore, they show higher durability and methanol tolerance when compared to the Pt catalysts.⁵⁰

Another hierarchically porous catalyst has been developed for ORRs. PS and anhydrous FeCl_3 were added to *N,N*-dimethylformamide (DMF) and stirred until a red solution was formed. This was then electrospun into fibres. After subsequent drying of these fibres, they were subjected to vapour phase polymerisation (VPP) with pyrrole for 12 hours. Following this, the fibres were heated at 900 °C for two hours in a nitrogen atmosphere. The inactive iron particles were then removed by acid leaching and then another identical heat treatment was performed and hierarchically porous iron and nitrogen doped carbon nanofibres were obtained. These were used to assemble a zinc-air battery which showed a higher power density and increased long-term stability when compared to a zinc-air battery produced using a commercial platinum catalyst.⁵²

Significant efforts have been made towards development of heterogeneous catalysts.⁵³ Stable surfaces have been shown to be unfavourable for catalysis whereas surfaces with defects or surfaces with high interfacial energy are more favourable.⁵⁴ Because of this, working with polymorphs of a material is an attractive method to tune catalytic activity. For oxidation of CO with an Au/TiO₂ catalyst, using a brookite TiO₂ polymorph instead of the anatase polymorph, complete oxidation occurs at significantly lower temperatures.⁵⁵

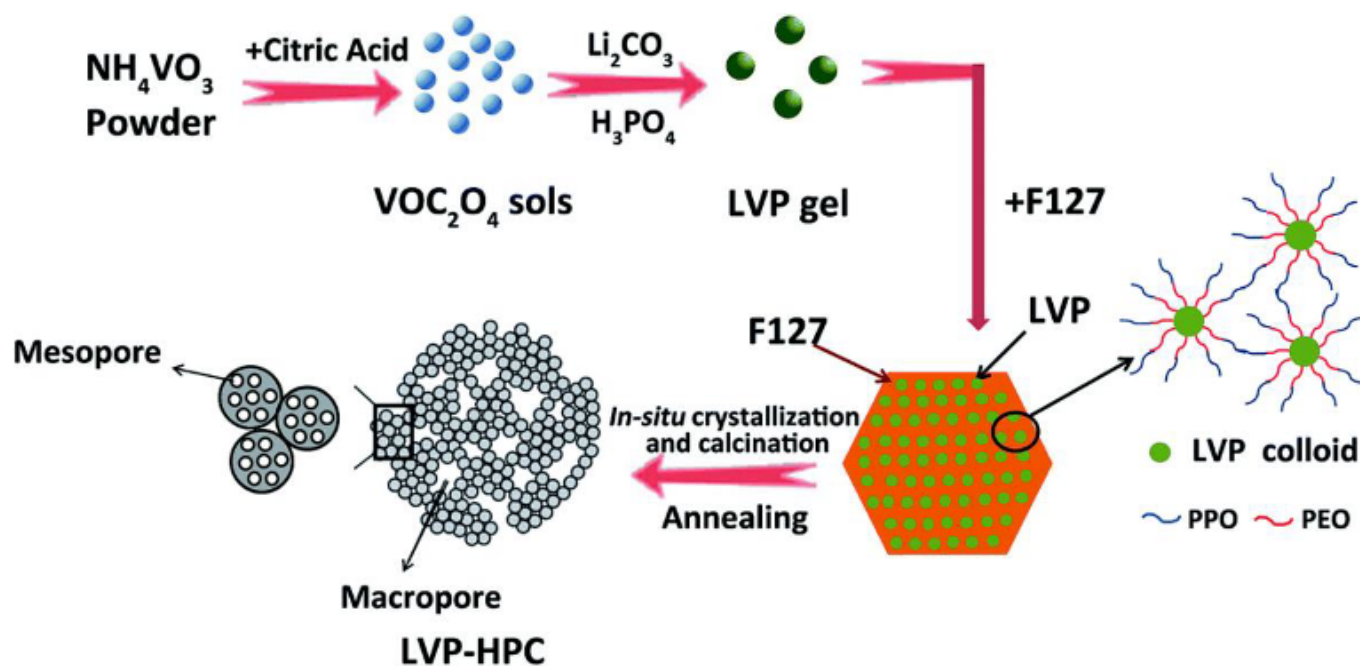


Figure 8. Schematic of the production of LVP-HPC. Reproduced with permission from Ref. 64. Copyright 2015, The Royal Society of Chemistry.

Alumina (Al_2O_3) is another common material used in catalytic processes.^{56,57} It is desirable due to being cheap, resistant to thermal and chemical treatment and has a high melting point.⁵⁸ Alongside the thermodynamically stable α - Al_2O_3 , there is also γ - Al_2O_3 which has a spinel structure with vacancies in the cation lattice.⁵⁹ It contains many Lewis acid sites on the surface which are employed in many catalytic processes.^{59–61} One study has produced an aerogel structure consisting of γ - Al_2O_3 . They reacted the volatile precursor trimethylaluminium (AlMe_3) with oxygen at a high temperature and in the gaseous phase. This obtained the kinetic product γ - Al_2O_3 instead of the thermodynamic product α - Al_2O_3 . It formed an aerogel-like structure with an interconnected micro-meso-macroporous network and its catalytic activity was investigated by using the dehydration of hexanol to 1-hexene as a model reaction. The γ - Al_2O_3 aerogel was far superior (91% conversion) to commercial γ - Al_2O_3 catalysts (29.5% conversion) and also showed a better selectivity.

Recently, there has been a number of novel developments of layer-like hierarchically structured and porous materials based on clays and layered silicates,¹⁵⁹ layered double hydroxides,^{160,161} 2D layered zeolites¹⁶² and others. The methods for their fabrication involve structural alteration and pore formation by pillaring and delamination. The role of the solvent in the processes of liquid exfoliation¹⁶³ of these types of layered materials involve various processes of absorption and swelling in the interlayer regions,¹⁶⁴ and solvent mediated recrystallization.¹⁶⁵ Due to their unique structuring, layered hierarchically porous materials have a range of potential applications in catalysis. A comprehensive recent review on the fabrication and application of layered hierarchically structured materials was recently published by Roth *et al.*¹⁶⁶

Energy storage, usage and conversion using hierarchically porous materials

Development of materials for more efficient energy storage, usage and conversion is a step towards replacing fossil fuels and multiple issues such as pollution, global warming and climate change.⁶² Lithium ion batteries have been a staple in the market of portable electronic devices for many years as their high energy density and durable cycle life makes them desirable. However, LiCoO_2 , the cathode material, is toxic, expensive and has lower specific capacity than the anode.^{63,64} Lately, lithium based phosphates have attracted a significant amount of attention as cathode materials.^{65,66} A recent hierarchically porous, lithium based phosphate that was produced was a composite of $\text{Li}_3\text{V}_2(\text{PO}_4)_3$ and carbon (LVP-HPC). It was produced as shown in Figure 8. This was then investigated for its suitability as an electrode and it was found to be robust, retaining 96% of its capacity after 800 cycles whereas the same material without the hierarchical structure retained only 81%. Furthermore, it exhibited high rate performance. These attributes have been explained by lower charge transfer resistance, increased diffusion rates of Li^+ and an interconnected, hierarchically porous structure with a large surface area.

Nanostructured materials with hierarchical porosity have been studied for solar and chemical energy conversion. Devices such as dye sensitised solar cells, solar cells, quantum dot solar cells and photocatalytic water splitting systems are of special interest due to harvesting clean solar energy.¹⁵⁴

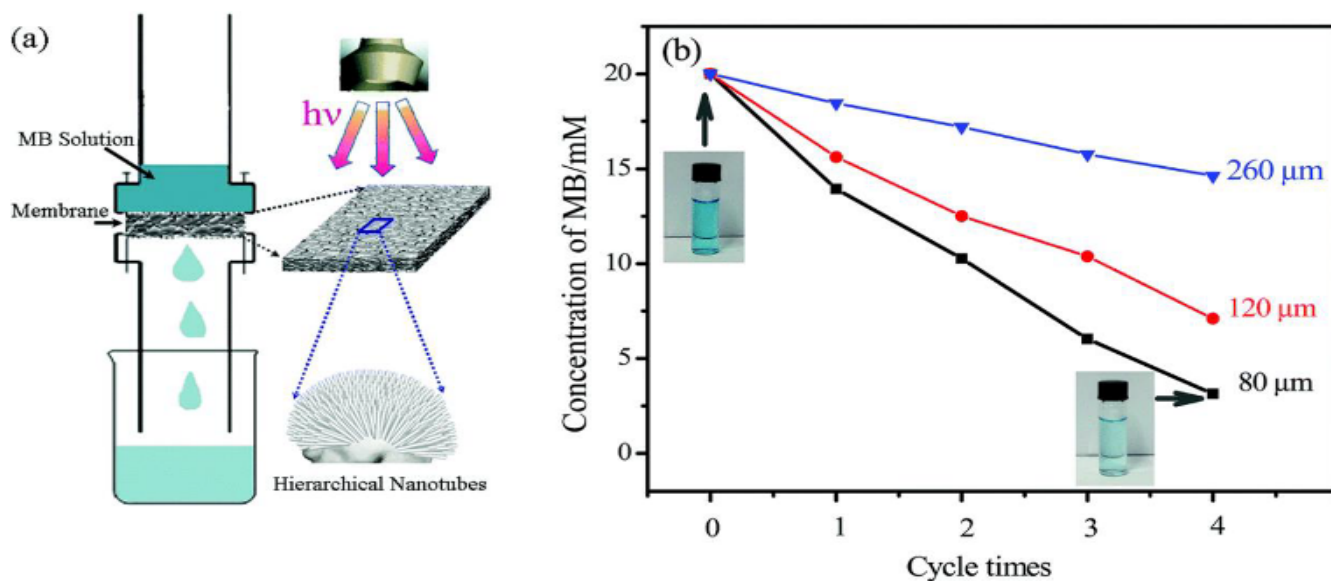


Figure 9. The flow-through photocatalysis set up can be seen in (a) and the reduction in MB concentration as a function of macropore size and number of cycles can be seen in (b). Reproduced with permission from Ref. 70. Copyright 2015, The Royal Society of Chemistry.

One group used beam assembly and lithography to produce hierarchically structured TiO_2 with various thickness of the macroporous structure and different sized mesopores (50 nm vs 90 nm).¹⁵⁵ N719 dye molecules were used to sensitise the hierarchically porous structures and the cell was assembled with a platinum coated counter electrode and an iodine/iodine-based electrolyte. It was found that the efficiency of the material with 50 nm mesopores was 4.5 times higher than the one with 90 nm mesopores. The thickness of the macroporous structure was also found to have an effect on the short circuit photocurrent density (J_{sc}). When the mesopores were 50 nm, increasing the thickness of the macroporous structure from 4 μm to 6 μm increased the J_{sc} from 7.29 mA cm^{-2} to 10.3 mA cm^{-2} . The authors stress the importance of the smaller mesopores adsorbing more dye due to the higher surface area and also mention why macropores are important to improve infiltration of electrolytes.

With fossil fuels being depleted at an alarming rate, efforts are being directed towards developing supercapacitors for energy storage. There are two types of supercapacitors: electrochemical double layer capacitors (EDLCs) and pseudocapacitors. They differ in their way of generating capacitance with EDLCs having capacitance produced by charge separation at the electrode/electrolyte interface. On the other hand, pseudocapacitors utilise reversible faradaic reactions occurring near or at an electrode surface.⁹ Low density polyethylene (LDPE) has been used recently to prepare hierarchically porous carbon spheres through autogenic pressure carbonisation.¹⁵⁶ The authors took LDPE powder and autoclaved at 600 $^\circ\text{C}$ for 30 minutes. Following this, it was activated with various amounts of KOH by heating to 700 $^\circ\text{C}$ under nitrogen for 1 hour. After washing with HCl (3.0) and deionized water and finally drying at 55 $^\circ\text{C}$ for 10 hours, hierarchically porous carbon spheres were obtained. They

showed that as the amount of KOH used was increased, they could control the hierarchically porous structures produced. These hierarchically porous carbon spheres were tested for their electrochemical performance and were found to have a high specific capacitance (355 F g^{-1} at 0.2 A g^{-1}) and good cycling efficiency, retaining 82.4% of its initial specific capacitance after 5000 cycles. Furthermore the energy and power densities reached 9.81 W h kg^{-1} and 450 W kg^{-1} , respectively. They attributed these properties to the presence of macropores that shorten electrolyte transfer distance, mesopores that accelerate electrolyte transport and micropores that provide abundant formation sites for the electric double layer.

Another group utilised a simple procedure to turn waste engine oil into hierarchically porous carbon nanosheets.¹⁵⁷ They mixed waste engine oil with concentrated sulfuric acid and then carbonised at 600–800 $^\circ\text{C}$ for 2 hours in an argon atmosphere. It was then mixed with KOH powder in various ratios, followed by heating to 700 $^\circ\text{C}$ for 1 hour under an argon atmosphere. The obtained hierarchically porous carbon nanosheets were washed with HCl and water and finally dried at 100 $^\circ\text{C}$ for 12 hours. Raman spectroscopy was used to gain some insights to the final material and it was found that they could control the amount of graphitisation by varying the temperature and amount of KOH used. This was important as the partially graphitised structure enhances the electronic conductivity and decreases the charge transfer impedance, hence leading to enhanced capacitive performance. Upon testing their electrochemical performance it was found that they could reach high specific capacitance (352 F g^{-1}) and retained up to 87.7% of initial capacitance when the current density was increased from 0.5 A g^{-1} to 20 A g^{-1} . Furthermore, they showed excellent cycling efficiency, retaining 99.6% of their specific capacity after 5000 cycles.

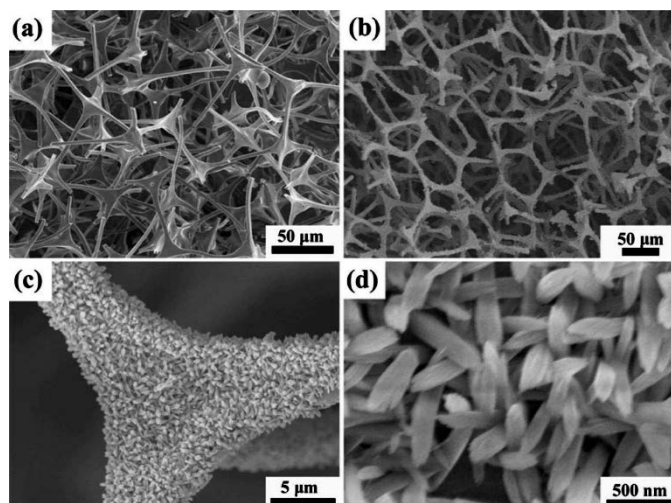


Figure 10. The carbon foam before the growth on β -FeOOH nanorods is shown in (a). (b) – (d) show the carbon foam with β -FeOOH nanorods grown directly onto the surface at different magnifications. Adapted with permission from Ref. 75. Copyright 2017, American Chemical Society.

Separation applications

Contamination of water as a by-product of human activity has been recognised as a serious environmental issue.^{67,68} Waste products from industrial processes which contain water immiscible oily compounds are common pollutants which has led to the investigation of materials that are efficient for separation of oil from water. Super-hydrophobic porous sponges with hierarchical structure have been produced by BF lithography and nanoparticle templating on an already macroporous polyurethane (PU) sponge. Poly(methyl methacrylate) (PMMA) and octadecyl-functionalised SiO_2 nanoparticles were mixed with a volatile solvent (THF). The PU sponge was soaked in this solution, followed by evaporation of THF in a moist environment. Due to water having a lower density than PMMA, the BF technique introduced surface roughness rather than porosity to the PMMA after evaporation of the water. The octadecyl-functionalised (hydrophobic) SiO_2 nanoparticles created a secondary roughness on the nanoscale. This hierarchical structure imparted superhydrophobicity which could be utilised for separation of oil and water and had very high oil absorption capacity (15 – 28 times its own weight). Furthermore, it was stable up to at least 115 °C and showed no significant reduction in absorption capacity after ten cycles (cleaned with purified oil or ethanol between each cycle). A final functionalisation of this hierarchically structured sponge was done by inclusion of magnetic nanoparticles in the initial formulation. Iron oxide nanoparticles were coated with SiO_2 which were again hydrophobically modified by functionalisation with octadecyl units. This allowed for manual targeting of oil pollutant through the use of a magnet. The sponge could also be cut into smaller pieces, increasing the area of contact between oil and sponge, then easily recovered using a magnet.⁶⁹ Fabrication of hierarchically porous titanium membrane was recently

reported by growth of TiO_2 nanotubes on macroporous titanium via anodization at 35 V with an aqueous hydrogen fluoride (HF) electrolyte. Drying of the membrane at 450 °C obtained the anatase polymorph of TiO_2 . Measurements showed that this membrane was super-hydrophilic in air and super-oleophobic whilst underwater and was efficient for separation of oil and water. The catalytic properties of anatase TiO_2 were exploited as a further functionality of the membrane (Figure 9). Methylene blue (MB) was used as a model pollutant and whilst the aqueous MB solution passed through the membrane, it was irradiated with UV light. A flow-through photocatalysis device was constructed which allowed investigation of the number of cycles and size of the macropores on the degradation of the MB. It was seen that the size of the macropores had a significant effect on the photocatalytic degradation of MB, with the membrane with the smallest macropores having an 84.5% reduction in MB concentration in the filtrate after four cycles. On the other hand, the membrane with the largest macropores had only a 27% reduction in MB concentration after four cycles. Finally, it was shown that after contamination of the membrane with the model pollutant octadecyltrimethoxysilane (OTS), the membrane could regain its functionality after irradiation with UV light.⁷⁰

Removal of pollutants

Environmental pollution is becoming a serious issue due to the rate at which large amounts of waste chemicals are being produced. The pollution of water with materials such as dyes and heavy metal ions can easily lead to them being taken in by the human body through consumption of contaminated water. Hierarchically porous materials are widely used for the sorption of harmful pollutants from the environment.⁹ Pollution of water with arsenic has become a worldwide issue and is hazardous to ecosystems and public health alike through accumulation in food chains. Materials such as active carbon, metal oxides, zeolites etc. have been investigated for their adsorption of As(III) and As(V), however, they have shown unsuitable uptake ability and low removal efficiencies.^{71–73} Iron-based materials have shown great promise for removal of arsenic by demonstrating enhanced capturing ability and a selective affinity for arsenic anions.⁷⁴

A hierarchically porous, functionalised carbon-based foam has been prepared and investigated for its arsenic removal ability (Figure 10). It was fabricated by a pyrolysis method with melamine foam as the starting material. The first step was heating at 700 °C for two hours, followed by hydrothermal treatment with nitric acid (3 M) at 120 °C for one hour. This hydrothermal treatment was done to impart hydrophilicity and maximise the presence of oxygen-containing functional groups. It was then washed and dried at 60 °C. The growth of β -FeOOH nanorods on the carbon foam was done by a further hydrothermal treatment. The foam was soaked in an aqueous solution of FeCl_3 , NaNO_3 , HCl and acetonitrile for one hour, followed by heating to 100 °C four hours. After washing and vacuum drying at 60 °C, the hierarchically porous carbon foam functionalised with β -FeOOH nanorods was obtained.⁷⁵ It was found to have smaller pore sizes and increased surface area when compared to the same material produced using a regular hydrothermal method. Both

materials were tested for their ability to adsorb Cu^{2+} ions and the one produced using the microwave assisted method performed better, demonstrating approximately a 20% reduction in concentration of Cu^{2+} compared to approximately 6.5% reduction. Furthermore, it showed a quicker rate of adsorption.⁷⁶ Upon investigating its ability to remove arsenic from water, it was found that it could reduce the concentration of a 10 ppm solution to less than 10 ppb which is the acceptable standard for drinking water set by the World Health Organisation (WHO). Through the use of Fourier transform infrared spectroscopy (FTIR) and x-ray photoelectron spectroscopy (XPS), they revealed the adsorption mechanism to be formation of As-O-Fe bonds and the replacement of hydroxyl radicals with H_2AsO_3^- and H_2AsO_4^- . The abundance of active sites due to the high surface area of the nanorods and the efficient mass transport due to the macroporous foam backbone leads to high adsorption of arsenic species.

One group utilised a microwave assisted hydrothermal method to produce hierarchically porous $\gamma\text{-Al}_2\text{O}_3$ from an aqueous solution of $\text{KAl}(\text{SO}_4)_2 \cdot 12\text{H}_2\text{O}$ and urea, followed by calcination at 600 °C. An interesting technique to fabricate hierarchically porous hydrogels involved exploitation of the well-known fermentation process that occurs when yeast and sugar are in water.

A pre-polymer solution was mixed with a solution of yeast and sugar in a sealed container and then polymerised. The production of CO_2 bubbles occurred and they were trapped within the already porous hydrogel matrix, obtaining a hierarchical structure that could be controlled by varying the concentrations of yeast and sugar. The produced hierarchically porous hydrogels showed increased swelling capacity and swelling rates as well as increased absorption of crystal violet (CV) dye, when compared to hydrogels produced without yeast and sugar.⁷⁷

Hierarchically structured materials for better sound absorption and sound insulation properties

Typical sound absorbing materials come in forms of polymer foams, fibres, boards, mats, perforated metals, aerogels and others.¹³²⁻¹³⁶ It has been recently suggested that introducing another level of porosity, e.g. dual porosity may enhance the acoustic absorption of porous materials.¹³⁷ Introduction of slits within aerated autoclaved concrete samples¹³⁸ showed to enhance acoustic absorption by a factor 1.5-2, as well as added holes in mineral wool.¹³⁹ Instead of hole-drilling, alternative approaches are to incorporate various particles, such as hemp,¹³⁹ reed¹⁴⁰ and polymer foam particles,¹⁴¹ within composite building materials in order to introduce different levels of porosity and improve the acoustic impedance of the material. Rutkevicius *et al.*^{123,124} produced porous cement and porous PDMS composites using a hydrogel templating technique and subsequent evaporation of the water from the hydrogels after the complete solidification of the cement or PDMS matrices. The porosity of the PDMS-hydrogel composites closely matched the content of the hydrogel in the samples, whereas in the cement-hydrogel composites the porosities were up to 10% lower compared to the corresponding hydrogel content. The samples were analysed using SEM and fibrous

domains were observed in the voids formed from the evaporated hydrogel. It was recently demonstrated that porous cement produced by this method has superior sound absorption coefficient for a range of sound frequencies than non-porous cement.^{124,125} The authors envisaged that the fibrous domains within the voids act as sound pressure dampeners, as the sound wave is transferred through the porous cement composite. PDMS composites showed a clear open-pore structure formation in the samples with >70 vol% hydrogel content. Such highly porous PDMS structures have sound absorption coefficient of 0.45-0.95 for the 70 vol% hydrogel-PDMS sample in the region 200-400 Hz and 0.4-0.8 in the region 1200-2000 Hz.

Thompson *et al.*¹²⁷ studied the sound transmission loss (STL) of hierarchically porous gypsum composites. They showed that the composites produced by the viscous trapping method had a lower sound transmission loss over the frequency range investigated as a function of the overall porosity. The effect of the composite pore size at a constant porosity on the sound transmission loss was also investigated. Their experiments showed that porous composites with large pores showed increased sound transmission loss at lower sound frequencies. As the sound frequency increased, the difference between their STL spectra decreased at the higher frequencies range (>2420 Hz), where the composites with smaller pores began to perform better. The hierarchically porous composite had an intermediate STL spectrum, suggesting a way for tailoring the hierarchically porous structure at constant porosity to achieve desired sound insulating properties at certain frequencies.

Smart soaps

Recently, the versatility of the hydrogel templating approach was demonstrated by developing novel pressure-responsive soap-hydrogel composites. The preparation steps for making porous materials were followed, however, the hydrogel bead template was not evaporated but left encased within the soap matrix.¹²⁸ These "smart" soap composites have a reduced cost, could reduce pollution with surface active materials and require less raw materials which improves the sustainability. The soap-hydrogel bead composites were stable for months in a standard soap packaging. These authors utilised agar hydrogel, a non-ionic gel with a high melting point, for the preparation of these composites (Figure 11). Upon chopping the hydrogel to beads of a desired size with a blender, controlled volume percentages of hydrogel bead slurry were mixed with molten soap. This mixture was then poured into a mould and allowed to harden before use. Interestingly, the authors found that upon compression a liquid can be released from the soap-hydrogel composite which can be used for pressure-triggered delivery of active components. For both PDMS and cement composites, high sound absorption coefficient in the low frequency range (200-400 Hz) was obtained, which makes these composites potential candidates as sound absorbing materials in sound dampening wall. They found that the soap dissolution rate increased with the volume percentage of hydrogel beads incorporated in the composite.

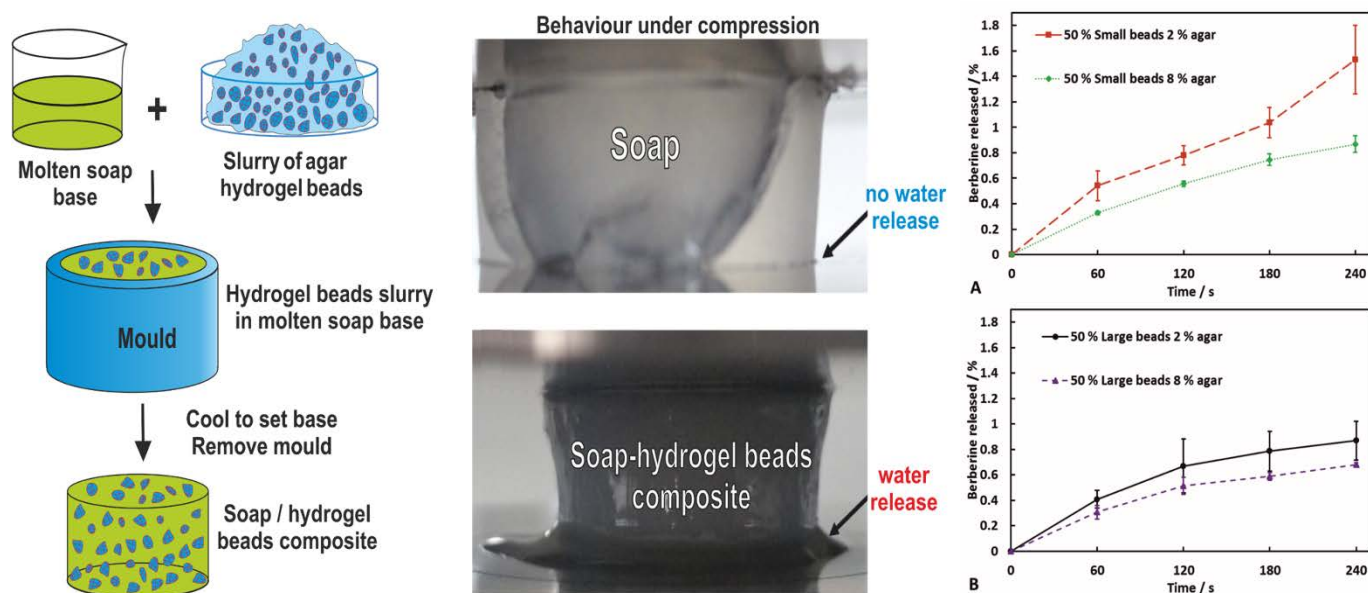


Figure 11. LHS: Schematics of the formulation of soap-hydrogel beads composites. Slurries of hydrogel beads are mixed with molten soap base in controlled volume ratios. The mixture was de-gassed to remove trapped air bubbles, poured into moulds and then refrigerated at 4 °C for 1 hour to set. MIDDLE: Digital camera images of a soap (TOP) and a soap hydrogel composite produced with 50% by volume of small hydrogel beads (BOTTOM) during compression. Note that the released water can be seen at the base of the composite. This effect is also seen when large hydrogel beads are used. The release rate of hydrogel-encapsulated active (berberine) from soap-hydrogel composites upon dissolution in water. RHS: The composites were produced using either small (A) or large (B) hydrogel beads prepared with different concentrations of agar. The percentage of released berberine has been monitored for soap composites with incorporated 50% by volume of hydrogel beads and initial concentration of berberine in the hydrogel beads of 0.15% w/v. Reproduced with permission from Ref. 128. Copyright 2018, The Royal Society of Chemistry.

The dissolution rate of composites with 50% by volume of hydrogel beads was 2.5 times faster than the soap control sample which they attribute this to an increase in the surface area of the soap bar exposed to water as hydrogel beads are detached from the surface of the composite. The release rate of species encapsulated within the hydrogel beads used in the composites was also investigated. It was found that the release rate of berberine could be increased almost two-fold by changing the size of hydrogel beads used from $600 \pm 300 \mu\text{m}$ to $120 \pm 60 \mu\text{m}$. The increase in surface area to volume ratio of smaller hydrogel beads, along with decreased diffusion path lengths and increased concentration gradients of berberine when using small hydrogel beads seems a plausible explanation for the observed difference in the release rates. The authors were also able to control the release rate of the encapsulated active by changing the agar concentration in the hydrogel. As the concentration of agar increased, the release rate decreased due to the formation of a denser polymer network, hindering the transport of the diffusing molecules. Another method to control the release rate of actives was to co-encapsulate an oppositely charged polyelectrolyte to attract the species. The release rate of the encapsulated active decreased as the concentration of the polyelectrolyte increased which these authors attribute to the ionic attraction between the polyelectrolyte and the diffusing active molecules, as well as the polyelectrolyte decreasing the free volume within the hydrogel

beads, thus hindering the molecular transport. The mechanical properties of the composites were investigated and found that the compressional strength decreased linearly with an increase in the volume percentage of hydrogel beads in the composite irrespective of the hydrogel bead size. The composites also showed a compression driven syneresis of water, suggesting that they could exercise washing action without running water. The Young modulus showed a significant increase when 5% or 7.5% by volume of hydrogel beads were incorporated within the composite. However, at higher volume percentages of beads, it decreased to values below the soap control sample.¹²⁸ The authors anticipate that such “smart” soap-hydrogel beads composites could find applications to increase sustainability within the hotel industry, where millions of partially used soap bars are discarded on a daily basis. The reduced cost of the smaller amount of soap base required for these materials combined with the possibility to encapsulate actives in the hydrogel beads content and the control of their release would make these composites appealing in personal care products.

Sensors

Development of sensors with rapid response times and low detection limits is essential for environmental monitoring, control of chemical processes and for occupational health and safety.

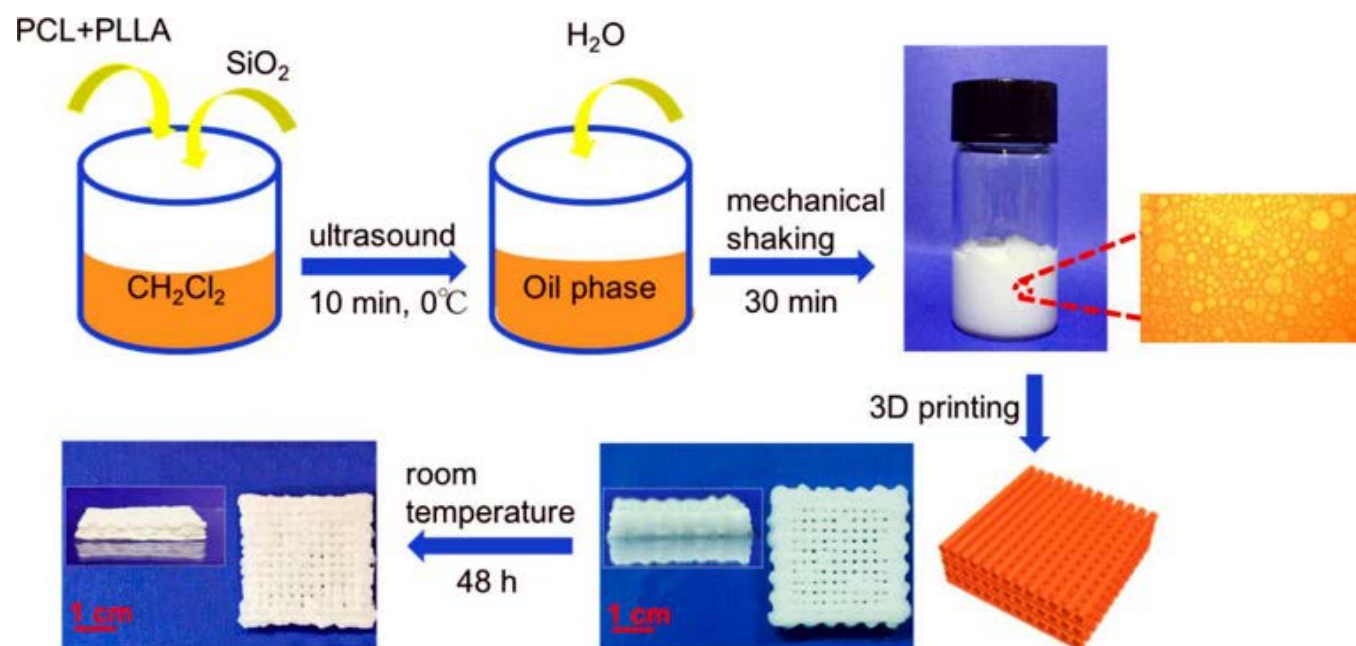


Figure 12. Schematic to show the formulation of a hierarchically porous biocompatible scaffold by 3D printing of a HIPE. Reprinted with permission from Ref. 89. Copyright 2017, American Chemical Society.

Due to the widespread use of organic liquids in many industrial processes, efforts must be made into the detection and subsequent automated intervention of solvent leaks. One study demonstrated the fabrication of a conductive polymer composite on a porous PU foam using a layer-by-layer (LbL) technique. The foam was dipped in a chitosan solution (positively charged) then the excess was removed, followed by dipping in a negatively charged solution of carbon black, cellulose nanocrystals and natural rubber. This was repeated for a number of times to obtain materials with different layer thicknesses and finally dried at 80 °C for six hours. It was tested for its detection ability using petroleum ether (PE) as a model organic liquid by connecting the produced material to two electrodes and monitoring its current signal over time before and after adding PE. The current signal showed a sharp decrease after addition of PE, with a response time of 0.05 – 0.15 s. The speed of the response was dependent on the thickness of the conductivity polymer composite on the PU foam, controlled by the number of LbL coatings. These response times are ~3 orders of magnitude faster than current state of the art sensors and are currently the fastest recorded in the literature. The rapid response of these composites has been attributed to the hierarchical structure, as when they were compared to bulk conductive polymer composites they were far superior. Furthermore, when organic liquids come into contact with the polymer coating, it causes swelling which blocks the micropores. Therefore, these materials are not only an efficient sensors, it can also block solvent leaks upon their detection.⁷⁸ Other work has developed a nitrogen doped hierarchically porous carbon that is an efficient sensor of uric acid (UA), dopamine (DA) and ascorbic acid (AA) in a 0.1 M PBS solution at physiological pH (7.4). These analytes were chosen as they play important roles in maintaining the functions of human

metabolism, the central nervous system and the circulatory system.⁷⁹ Its production began with a solvothermal treatment of aqueous ammonia solution, Zn(NO₃)₂·6H₂O, water, ethanol and 3-aminophenol at 100 °C for 24 hours. This yielded a resin which was washed and then subjected to two heat treatments; one at 550 °C followed by one at 1200 °C. After cooling, a 3D nitrogen doped hierarchically porous carbon was obtained. A glassy carbon electrode was then coated with this hierarchically structured material and tested for its ability to detect UA, DA and AA. Cyclic voltammetry demonstrated three separate, distinguishable anodic peaks representing UA, DA and AA and square wave voltammetry allowed for simultaneous detection and quantification of these analytes. It was suggested that the hierarchical structure, alongside an abundance of various functional groups was the reason this was possible.⁸⁰

Biomaterials

Introducing hierarchical porosity into materials for medical purposes has attracted much attention lately due to each level of porosity being functionalised to facilitate separate biological processes. For example, when preparing bioactive glasses for bone repair engineering, an interconnected macroporous network is a necessity as it allows for cell proliferation whilst ensuring effective mass transport between the growing tissue and surrounding media.⁸¹ Furthermore, a mesoporous network is desired due to being effective for drug release.⁸²

A hierarchically porous bioactive glass was prepared by first mixing commercial milk, SiO₂ nanoparticles and water in various ratios and then freeze-drying. Subsequent annealing at different temperatures between 600–800 °C in an air atmosphere yielded hierarchically porous bioactive glasses.

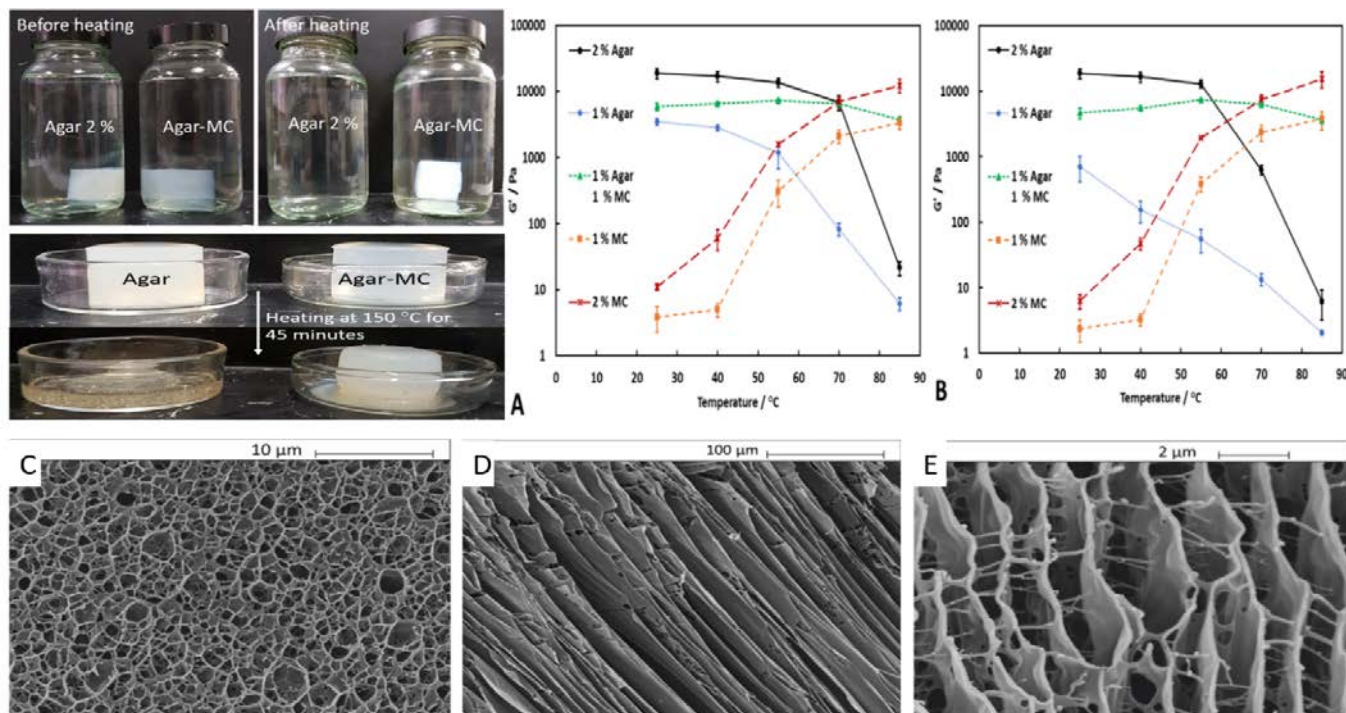


Figure 13. LHS-TOP: The image on the left shows hydrogel samples of agar (2.0% w/v) and Agar-MC (1.0% w/v – 1.0% w/v) immersed in water (200 cm³) before heating in the autoclave. The image on the right shows the samples after being heated in an autoclave at 121 °C and cooled down to room temperature. LHS-BOTTOM: These images show the agar hydrogel (2.0% w/v) and the composite Agar-MC hydrogel (1.0% w/v – 1.0% w/v) before (top) and after (bottom) heating in a furnace at 150 °C for 45 minutes. The agar gel melts, while the Agar-MC demonstrate melt-resistance. (A)-(B) The storage modulus of agar hydrogel (1.0% w/v and 2.0% w/v), MC (1.0% w/v and 2.0% w/v) and Agar-MC hydrogel (1.0% w/v – 1.0% w/v) as a function of temperature at shear stresses are 20 Pa (A) and 62 Pa (B). (C)-(E) SEM images of a flash-frozen and freeze-dried (C) agar (2.0% w/v) hydrogel sample, (D) MC (2.0% w/v) hydrogel sample and (E) Agar-MC hydrogel (1.0% w/v – 1.0% w/v) after it was flash-frozen in slush nitrogen, fractured by a blade and then sublimated at -70 °C for 7 minutes. Reproduced with permission from Ref. 129. Copyright 2017, The Royal Society of Chemistry.

Upon immersing the samples that were annealed at 600 °C in a simulated body fluid at 37 °C, hydroxyapatite began to form.⁸³ Bioactive glasses have also been shown to promote angiogenesis which is critical for wound healing due to oxygen and nutrient demands during the process.⁸⁴ The combination of electrospinning and pulsed laser deposition was used to produce a hierarchically structured bioactive glass which showed significantly increased wound healing abilities and re-epithelialisation when compared to materials without the hierarchical structure.⁸⁵ Fabrication of biocompatible and biodegradable materials for scaffolds should be performed with an aim to have a biodegradation rate similar to the rate of remodelling.⁸⁶ A water-in-oil HIPE stabilised by hydrophobic SiO₂ nanoparticles (h-SiO₂) was formulated that had a viscosity suitable for 3D printing. Water was added to a solution of poly(L-lactic acid) (PLLA) and poly(ϵ -caprolactone) (PCL) in dichloromethane (DCM) that contained h-SiO₂ nanoparticles. The final volume fraction of the dispersed water phase was 0.75. Through careful control of the pressure used during the 3D printing stage, the HIPE was stable to deformation and coalescence whilst being printed into a hierarchically structured scaffold which became porous after solvent evaporation (Figure 12). These biocompatible scaffolds were tested for their drug release kinetics, showing that the release rate of an anti-inflammatory drug was sufficient for combating inflammation in

the early period of implantation. The mechanism of drug release was investigated by fitting different kinetic models to the drug release profiles. It was shown that the Hixson-Crowell model was the most appropriate which describes a mechanism of drug erosion.⁸⁷ This model assumes spherical particles (that stay intact and spherical during dissolution) in perfect sink conditions i.e. no significant change in concentration of dissolved substance over time. It takes into account the change in surface area during dissolution.⁸⁸ Cell culture studies showed that the scaffold allowed for adhesion and proliferation of mouse bone mesenchymal stem cells (mBMSCs) which demonstrates their excellent biocompatibility.⁸⁹

Ultra-melt resistant composite hydrogel materials

Recently, a very interesting composite binary hydrogel system made from two food grade biopolymers, agar and methylcellulose (Agar-MC) which does not require addition of salt for gelation to occur, was found to have very unusual rheological and thermal properties.¹²⁹ It was found that the storage modulus of the Agar-MC hydrogel far exceeds those of hydrogels from the individual components (Figure 13). In addition, the Agar-MC hydrogel has enhanced mechanical properties over the temperature range 25–85 °C and a maximum storage modulus at 55 °C when the concentration of methylcellulose was 0.75% w/v or higher.

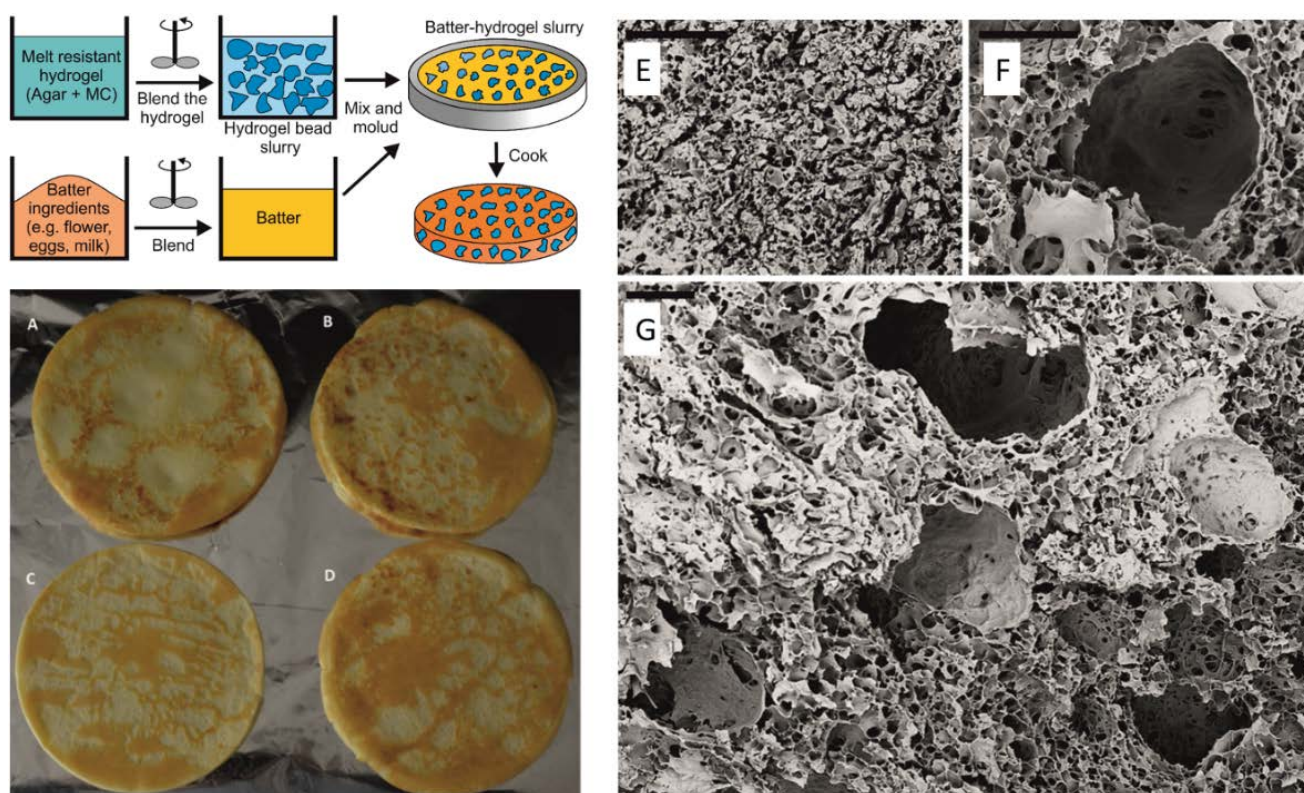


Figure 14. Top-left: Schematics of the process of templating batter with hydrogel slurries of highly melt-resistant hydrogel. Bottom-left: An optical photograph of a pancake (A) and pancake-hydrogel composites initially containing (B) 10%, (C) 17.5% and (D) 25% by volume slurry of Agar-MC hydrogel beads. These composites were produced with an initial volume percentage of 17.5% of Agar-MC hydrogel beads (1% w/v – 1% w/v). They were prepared by mixing a controlled volume percentage of slurry of hydrogel beads with pancake batter, then heating at 170 °C for 4 minutes on each side. SEM images of freeze-dried pancake (E) and pancake-hydrogel composites (F) and (G). The scale bars are all 100 μ m. Reprinted with permission from Ref.130. Copyright 2017, The Royal Society of Chemistry.

This was explained by a sol-gel phase transition of the methylcellulose upon heating as supported by differential scanning calorimetry (DSC) measurements. Above the melting point of agar, the storage modulus of Agar-MC hydrogel decreases but is still an elastic hydrogel with mechanical properties dominated by the MC gelation. By varying the mixing ratio of the two polymers, agar and MC, it was possible to engineer a food grade hydrogel of controlled mechanical properties and thermal response. SEM imaging of flash-frozen and freeze-dried samples revealed that the Agar-MC hydrogel contains two different types of heterogeneous regions of distinct microstructures. The latter was also tested for its stability towards heat treatment which showed that upon heating to temperatures above 120 °C its structure was retained without melting. The produced highly thermally stable hydrogel shows melt resistance which may find application in high temperature food processing and materials templating.¹²⁹

Structuring and caloric reduction in bakery products

Thompson *et al.*¹³⁰ recently combined the hydrogel templating methods with ultra-melt resistant hydrogels to design a new method for the reduction of caloric density in bakery products. They utilised a highly melt resistant hydrogel consisting of agar and methylcellulose. Upon blending of this mixed hydrogel, we

obtained a slurry of hydrogel microbeads (Figure 14). The authors have demonstrated this method on pancakes but its application to other bakery products is straightforward. Controlled volume percentages of slurry of hydrogel beads were mixed with pancake batter and cooked to produce pancake-hydrogel composites. The caloric densities of the composites were measured and when compared to a pancake control sample, they exhibited a reduction in caloric density comparable to the volume percentage of hydrogel beads initially incorporated within the composite. This method allowed controllable reduction of the caloric density up to $23 \pm 3\%$, when 25% by volume of hydrogel bead slurry was mixed with the pancake batter prior to cooking. We have analysed the microstructure of freeze-dried pancakes and pancake-hydrogel composites and the composites showed pores on a similar length scale to the hydrogel beads used, confirming that the hydrogel beads maintained their structure during the high temperature cooking process. Since this strategy is not limited to pancakes, one could expect it to find applications in a variety of food products such as waffles, crumpets, muffins, biscuits, cereal bars and many others. The authors suggest that this method could also be developed further by encapsulation of nutritionally beneficial or flavour enhancing ingredients within the hydrogel beads.¹³⁰

Conclusions and outlook

There are a range of methods in the literature that can be used for the preparation of hierarchically porous and structured materials. Furthermore, combinations of techniques can be employed to create structures on multiple length scales. They can be rationally designed for specific applications and functionalisation on each level of hierarchical structure is possible. The authors have been recently involved in this area by developing a range of hierarchically structured porous materials and composites based on the hydrogel bead templating and viscous trapping techniques. It has been shown how to control porosity, pore size, and ratio of large pores to small pores in a hierarchically porous material. The combination of hydrogel beads and other scaffolding materials can be further explored in terms of the development of better thermal insulation materials from sustainable resources. The future work related to sound transmission loss of porous structured materials could potentially involve testing of other hierarchically porous ceramics composites of different pore size distributions to see if it is possible to fine tune the sound insulation properties. Other work could involve investigation of the effect of the hydrogel residue. For example, variation of the gelling agent concentration would produce dried films with different mechanical properties and possibly obtain composite materials with different sound insulating properties. The research on smart soaps could involve soap-hydrogel bead composites for controlling the release rates of active species, like aromas or antimicrobials, encapsulated within these systems. It would be useful to see if the release rate of more widely used antimicrobials could be controlled in a similar fashion. Furthermore, investigation of the release rates during a simulated hand-wash could be performed to see if the composites would perform similarly in a more relevant situation. Future efforts should be directed at increasing the level of control over the ratio of different pore structures within the material i.e. vary the volume percentage of micropores and macropores at a constant porosity with an aim to fine-tune material properties. The study of such systems is highly interdisciplinary, as it is already the case for much of the research presented here, which needs a combined expertise from physics, materials chemistry, formulation science and biology.

Acknowledgements

B.R.T. acknowledges EPSRC Industrial CASE award and financial support from Unilever R&D Vlaardingen for his PhD studies.

Conflicts of Interests

There are no conflicts of interest to declare.

ORCID

Benjamin R. Thompson: 0000-0002-8309-9522

Tommy S. Horozov: 0000-0001-8818-3750

Simeon D. Stoyanov: 0000-0002-0610-3110

Vesselin N. Paunov: 0000-0001-6878-1681

References

- M. Rutkevicius, S. K. Munusami, Z. Watson, A. D. Field, M. Salt, S. D. Stoyanov, J. Petkov, G. H. Mehl and V. N. Paunov, *Mater. Res. Bull.*, 2012, **47**, 980–986.
- A. Feinle, M. S. Elsaesser and N. Hüsing, *Chem. Soc. Rev.*, 2016, **45**, 3377–3399.
- D. Schneider, D. Mehlhorn, P. Zeigermann, J. Kärger and R. Valiullin, *Chem. Soc. Rev.*, 2016, **45**, 3439–3467.
- W. J. Roth, B. Gil, W. Makowski, B. Marszalek and P. Eliasova, *Chem. Soc. Rev.*, 2015, 3400–3438.
- K. A. Cychoz, R. Guillet-Nicolas, J. Garcia-Martinez and M. Thommes, *Chem. Soc. Rev.*, 2017, **46**, 389–414.
- Q. Sun, Z. Dai, X. Meng and F.-S. Xiao, *Chem. Soc. Rev.*, 2015, **44**, 6018–6034.
- C. Z. Yuan, B. Gao, L. F. Shen, S. D. Yang, L. Hao, X. J. Lu, F. Zhang, L. J. Zhang and X. G. Zhang, *Nanoscale*, 2011, **3**, 529–545.
- M. Wang, X. Yu, Z. Wang, Z. Guo and L. Dai, *J. Mater. Chem. A*, 2017, **5**, 9488–9513.
- M.-H. Sun, S.-Z. Huang, L.-H. Chen, Y. Li, X.-Y. Yang, Z.-Y. Yuan and B.-L. Su, *Chem. Soc. Rev.*, 2016, **45**, 3479–3563.
- X.-Y. Yang, L.-H. Chen, Y. Li, J. C. Rooke, C. Sanchez and B.-L. Su, *Chem. Soc. Rev.*, 2017, **46**, 481–558.
- C. M. A. Parlett, K. Wilson and A. F. Lee, *Chem. Soc. Rev.*, 2013, **42**, 3876–3893.
- X.-Y. Yang, Y. Li, A. Lemaire, J.-G. Yu and B.-L. Su, *Pure Appl. Chem.*, 2009, **81**, 2265–2307.
- J. Rouquerol, D. Avnir, C. W. Fairbridge, D. H. Everett, J. H. Haynes, N. Pernicone, J. D. F. Ramsay, K. S. W. Sing and K. K. Unger, *Pure Appl. Chem.*, 1994, **66**, 1739–1758. 34.
- A. Vantomme, A. Léonard, Z. Y. Yuan and B. L. Su, *Colloids Surf., A*, 2007, **300**, 70–78.
- H. K. and Y. D. and H. S. and H. Deping, *J. Phys. D: Appl. Phys.*, 2011, **44**, 365405.
- H. Yu, A. Fisher, D. Cheng and D. Cao, *ACS Appl. Mater. Interfaces*, 2016, **8**, 21431–21439.
- P. Fratzl and R. Weinkamer, *Prog. Mater. Sci.*, 2007, **52**, 1263–1334.
- B.-L. Su, C. Sanchez and X.-Y. Yang, Insights into Hierarchically Structured Porous Materials: From Nanoscience to Catalysis, Separation, Optics, Energy and Life Science, in *Hierarchically Structured Porous Materials*, ed. B.-L. Su, C. Sanchez and X.-Y. Yang, Wiley-VCH Verlag GmbH & Co. KGaA, 2011, ch. 1, pp. 1–27.
- P. Colombo, C. Vakifahmetoglu and S. Costacurta, *J. Mater. Sci.*, 2010, **45**, 5425–5455.
- Ö. Sel and B. M. Smarsly, Hierarchically Structured Porous Materials by Dually Micellar Templating Approach, in *Hierarchically Structured Porous Materials*, ed. B.-L. Su, C. Sanchez and X.-Y. Yang, Wiley-VCH Verlag GmbH & Co. KGaA, 2011, ch. 3, pp. 41–53.
- R. Nagarajan, *Langmuir*, 1985, **1**, 331–341.
- O. Sel, D. Kuang, M. Thommes and B. Smarsly, *Langmuir*, 2006, **22**, 2311–2322.
- G. Widawski, M. Rawiso and B. Francois, *Nature*, 1994, **369**, 387–389.
- A. Zhang, H. Bai and L. Li, *Chem. Rev.*, 2015, **115**, 9801–9868.
- A. Boker, Y. Lin, K. Chiapperini, R. Horowitz, M. Thompson, V. Carreon, T. Xu, C. Abetz, H. Skaff, A. D. Dinsmore, T. Emrick and T. P. Russell, *Nat. Mater.*, 2004, **3**, 302–306.
- M. Srinivasarao, D. Collings, A. Philips and S. Patel, *Science*, 2001, **292**, 79–83.
- L. Qian and H. Zhang, *J. Chem. Technol. Biotechnol.*, 2011, **86**, 172–184.
- H.-W. Kang, Y. Tabata and Y. Ikada, *Biomaterials*, 1999, **20**, 1339–1344.
- M. L. Ferrer, R. Esquembre, I. Ortega, C. R. Mateo and F. del Monte, *Chem. Mater.*, 2006, **18**, 554–559.
- S. Deville, *Adv. Eng. Mater.*, 2008, **10**, 155–169.
- N. D. Petkovich and A. Stein, Colloidal Crystal Templating Approaches to Materials with Hierarchical Porosity, in *Hierarchically Structured Porous Materials*, ed. B.-L. Su, C. Sanchez and X.-Y. Yang, Wiley-VCH Verlag GmbH & Co. KGaA, 2011, ch. 4, pp. 55–129.

- 32 A. Stein, F. Li and N. R. Denny, *Chem. Mater.*, 2008, **20**, 649–666.
- 33 Y. Yin and Y. Xia, *Adv. Mater.*, 2001, **13**, 267–271.
- 34 O. D. Velev, T. A. Jede, R. F. Lobo and A. M. Lenhoff, *Nature*, 1997, **389**, 447–448.
- 35 M. Antonietti, B. Berton, C. Göltner and H.-P. Hentze, *Adv. Mater.*, 1998, **10**, 154–159.
- 36 P. Yang, T. Deng, D. Zhao, P. Feng, D. Pine, B. F. Chmelka, G. M. Whitesides and G. D. Stucky, *Science*, 1998, **282**, 2244–2246.
- 37 B. T. Holland, L. Abrams and A. Stein, *J. Am. Chem. Soc.*, 1999, **121**, 4308–4309.
- 38 O. D. Velev, P. M. Tessier, A. M. Lenhoff and E. W. Kaler, *Nature*, 1999, **401**, 548.
- 39 X. Li, J. Jiang, Y. Wang, X. Nie and F. Qu, *J. Sol-Gel Sci. Technol.*, 2010, **56**, 75–81.
- 40 S. D. Kimmins and N. R. Cameron, *Adv. Funct. Mater.*, 2011, **21**, 211–225.
- 41 V. O. Ikem, A. Menner and A. Bismarck, *Angew. Chem. Int. Ed.*, 2008, **47**, 8277–8279.
- 42 V. O. Ikem, A. Menner, T. S. Horozov and A. Bismarck, *Adv. Mater.*, 2010, **22**, 3588–3592.
- 43 L. L. C. Wong, P. M. Baiz Villafranca, A. Menner and A. Bismarck, *Langmuir*, 2013, **29**, 5952–5961.
- 44 S. Huš, M. Kolar and P. Krajnc, *Des. Monomers Polym.*, 2015, **18**, 698–703.
- 45 M. Sušec, S. C. Ligon, J. Stampfl, R. Liska and P. Krajnc, *Macromol. Rapid Commun.*, 2013, **34**, 938–943.
- 46 B. Zhao and M. M. Collinson, *Chem. Mater.*, 2010, **22**, 4312–4319.
- 47 M. Breulmann, S. A. Davis, S. Mann, H. P. Hentze and M. Antonietti, *Adv. Mater.*, 2000, **12**, 502–507.
- 48 L. Meng, X. Zhang, Y. Tang, K. Su and J. Kong, *Sci. Rep.*, 2015, **5**, 7910.
- 49 A. Kumar, F. Ciucci, A. N. Morozovska, S. V. Kalinin and S. Jesse, *Nat. Chem.*, 2011, **3**, 707–713.
- 50 Z. Hu, Z. Zhang, Z. Li, M. Dou and F. Wang, *ACS Appl. Mater. Interfaces*, 2017, **9**, 16109–16116.
- 51 J. Tang, R. R. Salunkhe, J. Liu, N. L. Torad, M. Imura, S. Furukawa and Y. Yamauchi, *J. Am. Chem. Soc.*, 2015, **137**, 1572–1580.
- 52 Y. Zhao, Q. Lai, Y. Wang, J. Zhu and Y. Liang, *ACS Appl. Mater. Interfaces*, 2017, **9**, 16178–16186.
- 53 A. Corma and H. García, *Chem. Rev.*, 2003, **103**, 4307–4366.
- 54 J. D. A. Pelletier and J.-M. Basset, *Acc. Chem. Res.*, 2016, **49**, 664–677.
- 55 W. Yan, B. Chen, S. M. Mahurin, S. Dai and S. H. Overbury, *Chem. Commun.*, 2004, 1918–1919.
- 56 Y. Men, H. Gnaser, R. Zapf, V. Hessel, C. Ziegler and G. Kolb, *Appl. Catal. A*, 2004, **277**, 83–90.
- 57 M. R. Avhad and J. M. Marchetti, *Catal. Rev.*, 2016, **58**, 157–208.
- 58 K. Hagedorn, U. Bahn Müller, A. Schachtschneider, M. Frei, W. Li, J. Schmedt auf der Günne and S. Polarz, *ACS Appl. Mater. Interfaces*, 2017, **9**, 11599–11608.
- 59 M. Trueba and S. P. Trasatti, *Eur. J. Inorg. Chem.*, 2005, **2005**, 3393–3403.
- 60 M. Trombetta, G. Busca, S. A. Rossini, V. Piccoli and U. Cornaro, *J. Catal.*, 1997, **168**, 334–348.
- 61 A. Zaherian, M. Kazemeini, M. Aghaziarati and S. Alamolhoda, *J. Porous Mater.*, 2013, **20**, 151–157.
- 62 S. Shafiee and E. Topal, *Energy Policy*, 2009, **37**, 181–189.
- 63 R. Zhang, Y. Zhang, K. Zhu, F. Du, Q. Fu, X. Yang, Y. Wang, X. Bie, G. Chen and Y. Wei, *ACS Appl. Mater. Interfaces*, 2014, **6**, 12523–12530.
- 64 Y. Cheng, W. Zhou, K. Feng, H. Zhang, X. Li and H. Zhang, *RSC Adv.*, 2017, **7**, 38415–38423.
- 65 Z.-X. Chi, W. Zhang, X.-S. Wang, F.-Q. Cheng, J.-T. Chen, A.-M. Cao and L.-J. Wan, *J. Mater. Chem. A*, 2014, **2**, 17359–17365.
- 66 J. Yang, J. Wang, Y. Tang, D. Wang, B. Xiao, X. Li, R. Li, G. Liang, T.-K. Sham and X. Sun, *J. Mater. Chem. A*, 2013, **1**, 7306–7311.
- 67 R. P. Schwarzenbach, B. I. Escher, K. Fenner, T. B. Hofstetter, C. A. Johnson, U. von Gunten and B. Wehrli, *Science*, 2006, **313**, 1072–1077.
- 68 M. A. Shannon, P. W. Bohn, M. Elimelech, J. G. Georgiadis, B. J. Marinas and A. M. Mayes, *Nature*, 2008, **452**, 301–310.
- 69 J. Zhang, Z. Meng, J. Liu, C. Schlaich, Z. Yu and X. Deng, *J. Mater. Chem. A*, 2017, **9**, 16369–16375.
- 70 L. Li, Z. Liu, Q. Zhang, C. Meng, T. Zhang and J. Zhai, *J. Mater. Chem. A*, 2015, **3**, 1279–1286.
- 71 X. Ge, J. Liu, X. Song, G. Wang, H. Zhang, Y. Zhang and H. Zhao, *Chem. Eng. J.*, 2016, **301**, 139–148.
- 72 W. Chen, R. Parette, J. Zou, F. S. Cannon and B. A. Dempsey, *Water Res.*, 2007, **41**, 1851–1858.
- 73 S. Shevade and R. G. Ford, *Water Res.*, 2004, **38**, 3197–3204.
- 74 Z. Wu, W. Li, P. A. Webley and D. Zhao, *Adv. Mater.*, 2012, **24**, 485–491.
- 75 X. Ge, Y. Ma, X. Song, G. Wang, H. Zhang, Y. Zhang and H. Zhao, *ACS Appl. Mater. Interfaces*, 2017, **9**, 13480–13490.
- 76 L. Nie, K. Deng, S. Yuan, W. Zhang and Q. Tan, *Mater. Lett.*, 2014, **132**, 369–372.
- 77 Q. Zhang, B. Chen, L. Tao, M. Yan, L. Chen and Y. Wei, *RSC Adv.*, 2014, **4**, 32475–32481.
- 78 X. Wu, Y. Han, X. Zhang and C. Lu, *Phys. Chem. Chem. Phys.*, 2017, **19**, 16198–16205.
- 79 J. Du, R. Yue, F. Ren, Z. Yao, F. Jiang, P. Yang and Y. Du, *Gold Bull.*, 2013, **46**, 137–144.
- 80 A. Nsabimana, J. Lai, S. Li, P. Hui, Z. Liu and G. Xu, *Analyst*, 2017, **142**, 478–484.
- 81 J. R. Jones, L. M. Ehrenfried and L. L. Hench, *Biomaterials*, 2006, **27**, 964–973.
- 82 X. Yan, C. Yu, X. Zhou, J. Tang and D. Zhao, *Angew. Chemie Int. Ed.*, 2004, **43**, 5980–5984.
- 83 D. Onna, Y. Minaberry and M. Jobbagy, *J. Mater. Chem. B*, 2015, **3**, 2971–2977.
- 84 M. N. Rahaman, D. E. Day, B. Sonny Bal, Q. Fu, S. B. Jung, L. F. Bonewald and A. P. Tomsia, *Acta Biomater.*, 2011, **7**, 2355–2373.
- 85 M. Xu, D. Zhai, L. Xia, H. Li, S. Chen, B. Fang, J. Chang and C. Wu, *Nanoscale*, 2016, **8**, 13790–13803.
- 86 K.-Y. Chen, W.-J. Liao, S.-M. Kuo, F.-J. Tsai, Y.-S. Chen, C.-Y. Huang and C.-H. Yao, *Biomacromolecules*, 2009, **10**, 1642–1649.
- 87 A. W. Hixson and J. H. Crowell, *Ind. Eng. Chem.*, 1931, **23**, 923–931.
- 88 J. Siepmann and F. Siepmann, *Int. J. Pharm.*, 2013, **453**, 12–24.
- 89 T. Yang, Y. Hu, C. Wang and B. P. Binks, *ACS Appl. Mater. Interfaces*, 2017, **9**, 22950–22958.
- 90 P. J. Flory, *Principles of Polymer Chemistry*, Cornell University Press, Ithaca, NY, 1953.
- 91 K. Almdal, J. Dyre, S. Hvidt and O. Kramer, *Polym. Gels Networks*, 1993, **1**, 5–17.
- 92 G. O. Phillips and P. A. Williams, 1 - Introduction to Food Hydrocolloids, in *Handbook of Hydrocolloids*, ed. G. O. Phillips and P. A. Williams, Woodhead Publishing Limited, Cambridge, 2nd edn., 2009, ch.1, pp. 1–22.
- 93 B. Xue, V. Kozlovska, F. Liu, J. Chen, J. F. Williams, J. Campos-Gomez, M. Saeed and E. Kharlampieva, *ACS Appl. Mater. Interfaces*, 2015, **7**, 13633–13644.
- 94 C. H. Araki, *J. Chem. Soc. Jpn.*, 1937, **58**, 1338–1350.
- 95 I. T. Norton, D. M. Goodall, K. R. J. Austen, E. R. Morris and D. A. Rees, *Biopolymers*, 1986, **25**, 1009–1029.
- 96 C. Araki, *Bull. Chem. Soc. Jpn.*, 1956, **29**, 543–544.
- 97 S. Arnott, A. Fulmer, W. E. Scott, I. C. M. Dea, R. Moorhouse and D. A. Rees, *J. Mol. Biol.*, 1974, **90**, 269–284.
- 98 I. C. M. Dea, A. A. McKinnon and D. A. Rees, *J. Mol. Biol.*, 1972, **68**, 153–172.
- 99 K. B. Guiseley, *Carbohydr. Res.*, 1970, **13**, 247–256.
- 100 K. C. Labropoulos, D. E. Niesz, S. C. Danforth and P. G. Kevrekidis, *Carbohydr. Polym.*, 2002, **50**, 407–415.
- 101 R. Armisén and F. Gaiatas, 4 - Agar, in *Handbook of Hydrocolloids*, ed. G. O. Phillips and P. A. Williams, Woodhead Publishing Limited, Cambridge, 2nd edn., 2009, ch. 4, pp. 82–107.
- 102 M. Leone, F. Sciortino, M. Migliore, S. L. Fornili and M. B. P. Vittorelli, *Biopolymers*, 1987, **26**, 743–761.
- 103 P. L. San Biagio, D. Bulone, A. Emanuele, M. B. Palma-Vittorelli and M. U. Palma, *Food Hydrocoll.*, 1996, **10**, 91–97.
- 104 S. Boral and H. B. Bohidar, *J. Phys. Chem. B*, 2012, **116**, 7113–7121.
- 105 J. C. F. Murray, 25 - Cellulosics, in *Handbook of Hydrocolloids*, ed. G. O. Phillips and P. A. Williams, Woodhead Publishing Limited, Cambridge, 2nd edn., 2009, ch. 25, pp. 710–723.
- 106 E. Heymann, *Trans. Faraday Soc.*, 1935, **31**, 846–864.
- 107 T. Kato, M. Yokoyama and A. Takahashi, *Colloid Polym. Sci.*, 1978, **256**, 15–21.
- 108 A. Haque and E. R. Morris, *Carbohydr. Polym.*, 1993, **22**, 161–173.
- 109 K. Kobayashi, C. Huang and T. P. Lodge, *Macromolecules*, 1999, **32**, 7070–7077.

- 110 S. A. Arvidson, J. R. Lott, J. W. McAllister, J. Zhang, F. S. Bates, T. P. Lodge, R. L. Sammler, Y. Li and M. Brackhagen, *Macromolecules*, 2013, **46**, 300–309.
- 111 J. R. Lott, J. W. McAllister, S. A. Arvidson, F. S. Bates and T. P. Lodge, *Biomacromolecules*, 2013, **14**, 2484–2488.
- 112 J. W. McAllister, J. R. Lott, P. W. Schmidt, R. L. Sammler, F. S. Bates and T. P. Lodge, *ACS Macro Lett.*, 2015, **4**, 538–542.
- 113 P. L. Nasatto, F. Pignon, J. L. M. Silveira, M. E. R. Duarte, M. D. Nosedo and M. Rinaudo, *Polymers*, 2015, **7**, 777–803.
- 114 J. Borreani, M. Espert, A. Salvador, T. Sanz, A. Quiles and I. Hernando, *Food Funct.*, 2017, **8**, 1547–1557.
- 115 D. Saha and S. Bhattacharya, *J. Food Sci. Technol.*, 2010, **47**, 587–597.
- 116 M. Tomšič, F. Prossnigg and O. Glatter, *J. Colloid Interface Sci.*, 2008, **322**, 41–50.
- 117 J. Bensted and S. P. Verma, *Cem. Technol.*, 1972, **3**, 67–70.
- 118 H.-J. Kuzel and M. Hauner, *Zement-Kalk-Gips*, 1987, **40**, 628–632.
- 119 M. E. Enayattallah, A. A. Khalil and A. M. Gadalla, *Trans. J. Br. Ceram. Soc.*, 1977, **76**, 95–104.
- 120 A. J. Lewry and J. Williamson, *J. Mater. Sci.*, 1994, **29**, 5279–5284.
- 121 A. J. Lewry and J. Williamson, *J. Mater. Sci.*, 1994, **29**, 5524–5528.
- 122 Y. W. I. Rahmanian, *Acta Polytech.*, 2009, **49**, 16–20.
- 123 M. Rutkevičius, S. K. Munusami, Z. Watson, A. D. Field, M. Salt, S. D. Stoyanov, J. Petkov, G. H. Mehl and V. N. Paunov, *Mater. Res. Bull.*, 2012, **47**, 980–986.
- 124 M. Rutkevičius, Z. Austin, B. Chalk, G. H. Mehl, Q. Qin, P. A. Rubini, S. D. Stoyanov and V. N. Paunov, *J. Mater. Sci.*, 2015, **50**, 3495–3503.
- 125 M. Rutkevičius, G. H. Mehl, V. N. Paunov, Q. Qin, P. A. Rubini, S. D. Stoyanov and J. Petkov, *J. Mater. Res.*, 2013, **28**, 2409–2414.
- 126 B. R. Thompson, T. S. Horozov, S. D. Stoyanov and V. N. Paunov, *Materials and Design*, 2018, **137**, 384–393.
- 127 B. R. Thompson, B. L. Taylor, Q. Qin, S. D. Stoyanov, T. S. Horozov and V. N. Paunov, *Mater. Chem. Front.*, 2017, **1**, 2627–2637.
- 128 B. R. Thompson, B. L. Taylor, Q. Qin, S. D. Stoyanov, T. S. Horozov and V. N. Paunov, *Mater. Chem. Front.*, 2018, **2**, 402–409.
- 129 B. R. Thompson, T. S. Horozov, S. D. Stoyanov and V. N. Paunov, *RSC Adv.*, 2017, **7**, 45535–45544.
- 130 B. R. Thompson, T. S. Horozov, S. D. Stoyanov and V. N. Paunov, *Food Funct.*, 2017, **8**, 2967–2973.
- 131 M. Rutkevičius, G. H. Mehl, J. T. Petkov, S. D. Stoyanov and V. N. Paunov, *J. Mater. Chem. B*, 2015, **3**, 82–89.
- 132 L.L. Beranek, I.L. VÉR IL, Noise and vibration control engineering: principles and applications. John Wiley & Sons, New York, 1992 New York.
- 133 T.J. Cox TJ, P. D'Antonio, Acoustic Absorbers and Diffusers: Theory, Design and Application. Taylor & Francis, London, 2004, UK
- 134 F.J. Fahy FJ Foundations of Engineering Acoustics. Elsevier Science, London, 2000, UK
- 135 J.P. Arenas, M.J. Crocker., *Sound Vib.*, 2010, **44**, 12–17.
- 136 D.-Y. Maa, *J. Acoust. Soc. of America*, 1998, **104**, 2861–2866.
- 137 X. Olny, C. Boutin, *J. Acoust. Soc. of America*, 2003, **114**, 73–89.
- 138 A. Laukaitis, B. Fiks, *Appl. Acoust.* 2006, **67**, 284–296.
- 139 N. Atalla, R. Panneton, F.C. Sgard, X. Olny, *J. Sound Vib.*, 2001, **243**, 659–678.
- 140 P. Glé, E. Gourdon, L. Arnaud, *Appl. Acoust.* 2011, **72**, 249–259.
- 141 S. Karabulut, M. Caliskan, *Proc. of Meetings on Acoustics*, 2013, **19**, 1–7.
- 142 D. Cuiyun, C. Guang, X. Xinbang, L. Peisheng, *Appl. Acoust.*, 2012, **73**, 865–871.
- 143 N. R. Cameron, *Polymer*, 2005, **46**, 1439–1449.
- 144 M. S. Silverstein, *Polymer*, 2017, **126**, 261–282.
- 145 Vargas L. and R. Q. Snurr, *Langmuir*, 2015, **31**, 10056–10065.
- 146 J.-M. Vanson, F.-X. Coudert, M. Klotz and A. Boutin, *Langmuir*, 2017, **33**, 1405–1411.
- 147 Y. Yi, X. Zheng, Z. Fu, C. Wang, X. Xu and X. Tan, *Materials (Basel)*, 2018, **11**, E380.
- 148 H. Shang, E. A. Olevsky and R. K. Bordia, *J. Am. Ceram. Soc.*, 2018, **102**, 1–10.
- 149 D. Wang, Z. Wang, Y. Li, K. Dong, J. Shao, S. Luo, Y. Liu and X. Qi, *Appl. Surf. Sci.*, 2019, **464**, 422–428.
- 150 M. S. Saleh, J. Li, J. Park and R. Panat, *Addit. Manuf.*, 2018, **23**, 70–78.
- 151 X. Y. Yang, L. H. Chen, Y. Li, J. C. Rooke, C. Sanchez and B. L. Su, *Chem. Soc. Rev.*, 2017, **46**, 481–558.
- 152 M. H. Sun, S. Z. Huang, L. H. Chen, Y. Lu, X. Y. Yang, Z. Y. Yuan and B. L. Su, *Chem. Soc. Rev.*, 2016, **45**, 3479–3563.
- 153 W. Schwieger, A. G. Machoke, T. Weissenberger, A. Inayat, T. Selvam, M. Klumppa and A. Inayata, *Chem. Soc. Rev.*, 2016, **45**, 3353–3376.
- 154 Y. Li, Z. Y. Fu, B. L. Su, *Adv. Func. Mater.*, 2012, **22**, 4634–4667.
- 155 C. Y. Cho and J. H. Moon, *Adv. Mater.*, 2011, **23**, 2971–2975.
- 156 H. Zhang, X. L. Zhou, L. M. Shao, F. Lu and P. J. He, *ACS Sustainable Chem. Eng.*, 2019, **7**, 3801–3810.
- 157 Y. Li, D. Zhang, J. He, Y. Wang, X. Zhang, Y. Zhang, X. Liu, K. Wang and Y. Wang, *Sustainable Energy Fuels*, 2019, **3**, 499–507.
- 158 R. Lakes, *Nature*, 1993, **361**, 511–515.
- 159 T. Selvam, A. Inayat and W. Schwieger, *Dalton Trans.*, 2014, **43**, 10365–10387.
- 160 R. Ma and T. Sasaki, *Acc. Chem. Res.*, 2015, **48**, 136–143.
- 161 L. Li, R. Z. Ma, Y. Ebina, K. Fukuda, K. Takada and T. Sasaki, *J. Am. Chem. Soc.*, 2007, **129**, 8000–8007.
- 162 W. J. Roth, P. Nachtigall, R. E. Morris and J. Čejka, *Chem. Rev.*, 2014, **114**, 4807–4837.
- 163 V. Nicolosi, M. Chhowalla, M. G. Kanatzidis, M. S. Strano and J. N. Coleman, *Science*, 2013, **340**, 1–18.
- 164 P. F. Luckham and S. Rossi, *Adv. Colloid Interface Sci.*, 1999, **82**, 43–92.
- 165 J. C. Vartuli, C. T. Kresge, M. E. Leonowicz, A. S. Chu, S. B. McCullen, I. D. Johnsen and E. W. Sheppard, *Chem. Mater.*, 1994, **6**, 2070–2077.
- 166 W. J. Roth, B. Gil, W. Makowski, B. Marszałek and P. Eliášová, *Chem. Soc. Rev.*, 2016, **45**, 3400–3438.